Margin Period of Risk in Credit Valuation Adjustment Calculations

Written by

Marco Kirana

Technical University Delft
Electrical Engineering, Mathematics and Computer Science

Supervised by

Prof. dr. ir. C.W. Oosterlee
Dr. R. Pietersz
Mr. M. Michielon MSc

For the degree of
Master in Applied Mathematics,
to de defended publicly on October 1, 2019

I would like to express my gratitude to my supervisors Dr. Raoul Pietersz and Matteo Michielon for their support and involvement in the project. I would also like to thank Prof. Kees Oosterlee for his feedback and help during the research period. Also, I want to thank Dr. Nestor Parolya for being part of my thesis committee.

Abstract

The aim of this thesis is to model fully collateralized exposures in the presence of the Margin Period of Risk, i.e., the time between the last successful collateral call to the time where the amount of the loss crystallizes. We start with introducing a closed-form expression to model fully collateralized exposures for fixed versus floating interest rate swaps. Then the Brownian bridge method is introduced and applied, which allows for improvements computational wise. Finally, fully collateralized exposures are modeled in the presence of the Margin Period of Risk, with the Least Squares Monte Carlo method in the case of one European call option under Black-Scholes assumptions.

Contents

Introduction

In this thesis we model *Credit Valuation Adjustment* in the case of having fully collateralized contracts between counterparties. In particular, we focus our analysis on the so called *Margin Period of Risk*, i.e., we model how exposure profiles behave between the time of the last successful collateral call and the time when the amount of the loss crystallizes. The main focus of the thesis is to be able to generate *expected positive exposure* profiles in the presence of the Margin period of Risk.

A general concept of Credit Valuation Adjustment is introduced in Chapter 1, where the definitions of expected positive exposure and Credit Valuation Adjustment are provided. Furthermore, agreement clauses like *netting* and *collateral* are discussed, which is used to reduce counterparty risk.

The Margin Period of Risk is modeled in Chapter 2. We consider a setting of having a portfolio consisting of one fixed versus floating interest rate swap. For this setting, we define a closed-form expression which provides insights and intuition behind the drivers of fully collateralized exposures. In terms of simulation, we make use of open source software, called *Open Source Risk Engine*. The Open Source Risk Engine allows us to generate an expected positive exposure profile in the presence of the Margin Period of Risk, where discounted portfolio values are obtained by crude Monte Carlo simulation. The expected positive exposure profile generated by the Open Source Risk Engine is used for comparison with the expected positive exposure profile generated with our closed-form expression. We then introduce a method called the *Brownian bridge method*, which results in obtaining discounted portfolio values without having to resort to brute-force daily crude Monte Carlo simulation of these portfolio values. This method can be useful when we deal with large portfolios, where calculating discounted portfolio values on a daily basis is computationally expensive. Again we make use of the Open Source Risk Engine, where we compare both expected positive exposure profiles obtained with the Open Source Risk Engine and the Brownian bridge method in terms of how accurate the Brownian bridge method is.

In Chapter 3, the Margin Period of Risk is modeled in the setting where

discounted portfolio values are approximated by the *Least Squares Monte Carlo* method. In this method, regression functions are used to approximate discounted portfolio values at every path and every time step. These approximated discounted portfolio values are used to generate an expected positive exposure profile. We work in a standard Black-Scholes setting, with a portfolio that only contains one European call option. In order to model the Margin Period of Risk, we first analyze the setting where there is no collateralization. We then expand this setting to the fully collateralized setting, where we show results and compare the expected positive exposure profiles obtained by the Least Squares Monte Carlo method with the expected positive exposure profile obtained by Black-Scholes.

In the last chapter, Chapter 4, we state all our findings and suggest further directions of research.

Chapter 1

An overview on Credit Valuation Adjustment

Until the financial crisis of 2008, many (if not all) aspects of counterparty credit risk, i.e., the possibility that a counterparty will not honor its contractual obligations, were often overlooked in common derivative valuation practices. Therefore, to provide a fair-value adjustment where counterparty credit risk is assessed, banks now make use of *Credit Valuation Adjustment* (CVA).

In this section we provide a general overview of the framework we are going to make use of to correctly estimate counterparty credit risk for derivative valuations. In particular, we mainly follow the approach outlined in [1] (see Chapter 2 therein). For the sake of clarity, as this framework is used for valuation purposes only, from here onwards we will be always working with a (naturally) filtered probability space $(\Omega, (\mathscr{F}(t))_{t\in[0,T]}, \mathbb{Q})$, where $\mathbb{Q}$ denotes the risk neutral measure.

Given a (portfolio/netting-set of) contract(s) between a bank B and a counterparty C (we conventionally assume that a positive amount represents a credit for B, while a negative one a debit), the following notation will be used from this point forward:

T	Longest amongst the maturities in the portfolio;
t	Time variable ($t \in [0, T]$);
$\Pi(t, T)$	Sum of all the discounted (at time t) cash flows linked to the portfolio occurring between t and T (both t and T included);
$\mathbb{E}_t[\cdot]$	$\mathbb{Q}$-expectation conditional to the σ-algebra $\mathscr{F}(t)$. For convenience, in the case of $t = 0$ or when $\mathscr{F}(t)$ is specified in the $\mathbb{Q}$-expectation, the subscript will be left out;
Rec	Recovery rate of the counterparty;

τ	(Random) default time of the counterparty;
LGD	Loss given default of the counterparty, i.e., LGD = 1 - Rec;
$\mathrm{PD}(t_{i-1}, t_i]$	Probability of default in the interval $(t_{i-1}, t_i]$;
$P(0,t)$	Discount factor from t to 0;
$\max(\cdot, 0)$	Positive part of the quantity within brackets. In the case of having to deal with extensive formulas, $(\cdot)^+$ is used;
$V(t)$	Value of the portfolio at time t, i.e., $V(t) = \mathbb{E}_t[\Pi(t,T)]$;
$\mathbb{1}_{\{\cdot\}}$	Indicator function of the event $\{\cdot\}$.

1.1 (Unilateral) CVA

According to [1] (see Section 2.3 therein), (Unilateral) CVA (i.e., UCVA) can be defined as the difference between the risk-free portfolio value and the portfolio value that takes into account the possibility of the counterparty defaulting. Since the financial crisis, CVA became a central part of counterparty risk management. Furthermore, CVA can also be used to manage, price and hedge counterparty risk. To avoid ambiguity, from here onwards amounts are always seen from the point of view of B. Further, we will be always assuming that a portfolio per as per Section 1 is considered.

We start with deriving the formula of *exposure*, which is the amount B can lose, should C default. According to [2], the exposure B has with respect to C is determined in the following way: if the contract value is *negative* for B when C defaults, then B closes out the position by paying C the market value of the contract. B has, thus, a net loss of zero. If the contract value is *positive* for B when C defaults, then B closes out the position and receives nothing from the counterparty. B has, thus, a net loss equal to the market value of the contract. We conclude that the exposure is either zero or the market value of the contract, thus exposure is given by

$$\mathrm{E}(t) = \max(V(t), 0), \tag{1.1}$$

of which only a fraction is actually recovered if C defaults, denoted by the *recovery rate* Rec (which is the share of an asset that is recovered if a borrower defaults). Now we define the *expected positive exposure* (EPE) (uncollateralized case), which is the risk neutral discounted expectation of the exposures:

$$\begin{aligned} \mathrm{EPE}(t) &= \mathbb{E}[P(0,t) \cdot \max(V(t), 0)] \\ &= \mathbb{E}[P(0,t) \cdot \mathrm{E}(t)]. \end{aligned} \tag{1.2}$$

Obtaining values for the EPE at different times $t \in [0, T]$ results in an *EPE profile*. Therefore, it is natural to define CVA as the expectation at time 0 of the discounted exposures at default time τ, multiplied with the *Loss Given Default* (LGD), i.e.,

$$\text{CVA} = \mathbb{E}\big[\text{LGD} \cdot \mathbb{1}_{\{\tau<T\}} \cdot P(0,\tau) \cdot \text{E}(\tau)\big]. \tag{1.3}$$

Note that the LGD (which is the share of an asset that is lost if a borrower defaults, defined as 1 - Rec) is chosen to be constant in (1.3) for simplicity. Following [3] (Section 2.1 therein), if we assume that τ is independent of other processes, and that we have partitioned the interval $[0, T]$ in the partition $0 < t_1 < \ldots < t_n = T$, we can approximate the formula of CVA in (1.3) as

$$\text{CVA} \approx \text{LGD} \cdot \sum_{i=1}^{n} \mathbb{Q}[t_{i-1} < \tau \leq t_i] \cdot \text{EPE}(t_i), \tag{1.4}$$

where $\mathbb{Q}[t_{i-1} < \tau \leq t_i]$ (or $\text{PD}(t_{i-1}, t_i]$) is the risk neutral probability of the default of counterparty C in the interval $(t_{i-1}, t_i]$. Letting $n \to \infty$ in (1.4) (resulting in a grid with an infinite amount of grid points) causes the approximation sign to turn into a equality sign.

1.2 Reducing counterparty risk

Counterparties often attempt to reduce credit risk, despite that this type of risk cannot be completely eliminated. In this section we consider two agreement clauses aimed to reduce counterparty risk, i.e, *netting* and *collateral*.

1.2.1 Netting

According to [2], netting can be described as an agreement between two counterparties that, in the event of default, allows aggregation of transactions between them. This means that transactions with a negative value can be used to offset transactions with positive value. If B has two contracts with C with (t-discounted) portfolio values $\Pi^{(1)}(t, T)$ and $\Pi^{(2)}(t, T)$, respectively, and no netting agreements in place in the case of default of C, then B would lose

$$\text{LGD} \cdot \big(\max(\mathbb{E}[\Pi^{(1)}(\tau, T)|\mathscr{F}(\tau)], 0) + \max(\mathbb{E}[\Pi^{(2)}(\tau, T)|\mathscr{F}(\tau)], 0)\big). \tag{1.5}$$

With netting on the other hand, B would lose

$$\mathrm{LGD} \cdot \max\big(\mathbb{E}[\Pi^{(1)}(\tau, T)|\mathscr{F}(\tau)] + \mathbb{E}[\Pi^{(2)}(\tau, T)|\mathscr{F}(\tau)], 0\big). \tag{1.6}$$

Note that (1.5) is never smaller than (1.6), due to the convexity of the maximum function, which shows that netting mitigates counterparty risk.

1.2.2 Collateral

In [1] (Section 2.5 therein), collateral (or margin) is described as an asset of the borrower that is transferred to the lender if the borrower defaults. After the default, the lender becomes the owner of the collateral. Collateral creates protection towards the lender, which results in a reduction of counterparty risk compared to a contract with no collateral. In the case of fully collateralization and no collateral thresholds, collateral must be kept in line with the Mark-to-Market (fair value) of the portfolio of deals with the counterparty. When the mark-to market is negative to B, B has to post collateral. Conversely, when the mark-to-market is positive to B, then C has to post collateral.

In this framework we assume that counterparties make use of a *Credit Support Annex* (CSA), which is a legal document aimed to offer credit protection by setting up rules in terms of (mutual) posting of collateral. Aspects included in a CSA are:

- Collateral posting thresholds, which define maximum amounts of exposures before a party is required to post collateral;
- Minimum Transfer Amounts (MTA's), i.e., thresholds that establish the minimum valid amount of margin before a party needs to post collateral;
- Rounding collateral movements to some reasonable unit;
- Frequency of portfolio revaluation and collateral rebalancing.

The last feature is connected to determining the start of the "Margin Period of Risk", which will be discussed in Chapter 2.

1.3 CVA modeling

In this section we briefly outline the steps involved in CVA calculations, and the challenges that can arise, as highlighted in [4] (see Section 6.1 therein). In general, the following intuitive steps are involved:

(1) Simulation of market risk variables.

(2) Evaluation of all contract values belonging to the portfolio for every path and every time step.

(3) Aggregation of all contract values for every path and every time step in the simulation.

(4) Application of the CSA contract features.

(5) Estimate the PD at every observation date (assuming the LGD is kept constant).

(6) Calculation of CVA, with the formula stated in (1.4).

We can see that we need to valuate each contract for every path and every time step, which is computationally very expensive. We would have to reduce the amount of time steps, reduce the amount of simulated paths or reduce the complexity of the models used for valuation, which causes the accuracy of the computation of CVA to decrease. In Chapter 2, brute force simulation of portfolio values (i.e. crude Monte Carlo) is used, which is acceptable because our framework is used for testing purposes only. In Chapter 3, a different method is used to obtain portfolio values (Least Squares Monte Carlo), where these values are approximated at every path and every time step by making use of regression functions.

Chapter 2

Modeling Margin Period of Risk

To model collateralized exposures we have to acknowledge that the default of a counterparty cannot be considered as a one-time event, but as an entire sequence of events leading up to and following the default itself. This sequence of events we are going to model defines a period of time called the *Margin Period of Risk* (MPoR). In particular, we mainly follow the approach outlined in [5], where the MPoR is described as the time from the last successful margin call (the last successful posting of collateral) before the eventual default to the time when the amount of the loss crystallizes (when the contract with the counterparty is terminated).

Note that we are not interested in modeling the duration of the MPoR, which is assumed to be constant, but instead we focus on generating EPE profiles in the presence of the MPoR.

There are two possible types of margin, i.e., *initial margin* and *variation margin*. Our framework focuses on variation margin (VM), which means that the amount of collateral that needs to be posted is regularly adjusted. Relating to the margining frequency, daily remargining is assumed in our framework.

Furthermore, we assume in our framework that exposures are collateralized fully, which means that the amount of collateral that needs to be posted on a daily basis is equal to the exposure on that day.

In this chapter we start with introducing some fundamental terms when modeling exposures, then we take a look at a closed-form expression to obtain an EPE profile of a portfolio consisting of a single fixed versus floating interest rate swap, and at last we implement a method called *The Brownian bridge method*. On top of the notation already introduced in Chapter 1, we define the following symbols:

$A_B(t)$	Collateral amount B needs to post at time t;
$A_C(t)$	Collateral amount C needs to post at time t;
$c(t)$	Total collateral amount at time t in possession of B;
h_B	Collateral posting threshold for B;
h_C	Collateral posting threshold for C;
δ	The Margin Period of Risk;
$y(t)$	Forward swap rate at time t;
N	Notional amount;
$\bar{T}_i^{\text{fix}}$	The i-th fixed cash flow;
$\bar{T}_i^{\text{flt}}$	The i-th floating cash flow;
τ_i^{fix}	Accrual factor between the i-th and the $(i-1)$-th fixed cash flow;
τ_i^{flt}	Accrual factor between the i-th and the $(i-1)$-th floating cash flow;
$F(t, T_1, T_2)$	Forward rate at time t, in the period $[T_1, T_2]$;
$\text{pvbp}_{i(u)}(t)$	Present value of a basis point at time t, with observation date u fixed, for fixed cash flows that occur after u;
$M(t)$	Numeraire at time t, $M(t) := \frac{1}{P(0,t)}$;
$\sigma(t)$	Volatility at time t;
$W(t)$	Wiener process/Brownian motion at time t;
$\mathcal{N}(\mu, \sigma^2)$	Normal distribution with mean μ and variance σ^2.

2.1 Fundamental definitions

In this section we will provide some fundamentals to model exposures in the presence of collateralization (see [5], Sections 2.1 and 2.2 therein). The *exposure* at time t in the collateralized case is similar to (1.1), but the collateral amount is subtracted from the market value of the contract, i.e.,

$$\text{E}(t) = \max(V(t) - c(t), 0), \quad c(t) = A_C(t) - A_B(t). \tag{2.1}$$

Furthermore, each party can have *collateral posting thresholds*, which will change the value of collateral that B or C needs to post at time t to

$$A_B(t) = \max(-V(t) - h_B, 0), \qquad A_C(t) = \max(V(t) - h_C, 0). \tag{2.2}$$

A *margin call* is used when $A_B(t)$ or $A_C(t)$ needs to be adjusted. In reality, these adjustments take several days to complete. In our framework we make use of daily remargining, which results in the event of overlapping margin calls.

There are two types of payments, i.e., *trade flows* and *margin flows*. Trade

flows are cash flows (can also be other asset transfers) connected to the trade themselves, and margin flows are payments in terms of the posting of collateral between parties. Partially missing a margin flow is a common occurrence, and an event that causes these partial payments are called *disputes*, i.e, disagreements between parties concerning the amount of collateral that needs to be posted. These disputes may result in a longer period of time between the last fully settled margin call and the possible termination of a portfolio.

2.2 Closed-form expression for interest rate swaps

In this section we introduce a closed-form expression to model fully collateralized exposures for fixed versus floating interest rate swaps. Let u be an observation date, which is chosen fixed per model. This model is created only for the time interval $[0, u]$, where the MPoR is displayed in the period $[u - \delta, u]$. By letting the observation dates vary from 0 to T (having a different model every time), we are able to model the MPoR for every observation date.

We assume that during the MPoR, there are no cash flows. The reason behind this is because when a counterparty fails to post collateral, we assume that the bank will detect this and freezes outgoing payments to that specific counterparty. See Figure 2.1 for an illustration of the model.

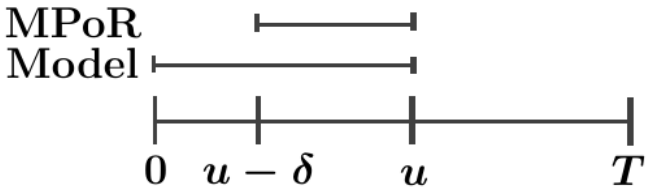

Figure 2.1: The model is created for the time interval $[0, u]$, where the Margin Period of Risk occurs in the time interval $[u - \delta, u]$

Note that because of our assumption that there are no cash flows during the MPoR, we only have to focus on cash flows occurring after time u, in terms of modeling the MPoR.

Let us consider a fixed (pay) versus floating (receive) interest rate swap, with fixed rate K and maturity T. Furthermore, assume this swap has an n amount of fixed cash flows and an m amount of floating cash flows that occur

in $(u, T]$. The sum of fixed cash flows occurring after time u and discounted back to time t is described as

$$K \cdot \sum_{j=i(u)}^{n} \tau_j^{\text{fix}} \cdot P(t, \bar{T}_j^{\text{Fix}}),$$

where $P(t, \bar{T}_j^{\text{Fix}})$ is the discount factor from time $\bar{T}_j^{\text{Fix}}$ to time t and τ_j^{fix} the corresponding accrual factor. $i(u) = \min_i\{\bar{T}_i^{\text{fix}} > u\}$ is the index of the first fixed cash flow occurring after time u. The sum of floating cash flows occurring after time u and discounted back to time t is described as

$$\sum_{j=k(u)}^{m} \tau_j^{\text{flt}} \cdot F(t, \bar{T}_{j-1}^{\text{flt}}, \bar{T}_j^{\text{flt}}) \cdot P(t, \bar{T}_j^{\text{flt}}),$$

where $F(t, \bar{T}_{j-1}^{\text{flt}}, \bar{T}_j^{\text{flt}})$ is the forward rate at time t, in the period $[\bar{T}_{j-1}^{\text{flt}}, \bar{T}_j^{\text{flt}}]$. $k(u) = \min_k\{\bar{T}_k^{\text{flt}} > u\}$ is the index for the first floating cash flow occurring after time u.

We have for the value at time t (time variable of the model) with $0 \leq t \leq u$, observation date u fixed, of cash flows occurring after u that

$$V(t) = N \cdot (y(t) - K) \cdot \text{pvbp}_{i(u)}(t), \tag{2.3}$$

where

$$y(t) = \frac{\sum_{j=k(u)}^{m} \tau_j^{\text{flt}} \cdot F(t, \bar{T}_{j-1}^{\text{flt}}, \bar{T}_j^{\text{flt}}) \cdot P(t, \bar{T}_j^{\text{flt}})}{\text{pvbp}_{i(u)}(t)}, \tag{2.4}$$

and

$$\text{pvbp}_{i(u)}(t) = \sum_{j=i(u)}^{n} \tau_j^{\text{fix}} \cdot P(t, \bar{T}_j^{\text{fix}}). \tag{2.5}$$

See Appendix A for the value of cash flows occurring after u in (2.3), rewritten to a sum of fixed and floating legs.

Note that $\text{pvbp}_{i(u)}(t)$ is just the sum of discount factors at the fixed cash flow dates after time u, discounted back to time t (and multiplied each with their respective accrual factor).

The variable $y(t)$ is the *forward swap rate*, which is the value of the fixed rate at time t, for an interest rate swap with payments occurring after time u, such that the value of the interest rate swap at time t is equal to zero. We

can see this by setting $y(t)$ in (2.4) equal to the fixed rate K:

$$y(t) = K$$

if and only if

$$\sum_{j=k(u)}^{m} \tau_j^{\text{flt}} \cdot F(t, \bar{T}_{j-1}^{\text{flt}}, \bar{T}_j^{\text{flt}}) \cdot P(t, \bar{T}_j^{\text{flt}}) = K \cdot \text{pvbp}_{i(u)}(t)$$

if and only if

$$\sum_{j=k(u)}^{m} \tau_j^{\text{flt}} \cdot F(t, \bar{T}_{j-1}^{\text{flt}}, \bar{T}_j^{\text{flt}}) \cdot P(t, \bar{T}_j^{\text{flt}}) = K \cdot \sum_{j=i(u)}^{n} \tau_j^{\text{fix}} \cdot P(t, \bar{T}_j^{\text{fix}}). \tag{2.6}$$

If the equality in (2.6) holds, the value of the interest rate swap is equal to zero, because of the sum of fixed cash flows and the sum of floating cash flows being equal. This result could also be simply obtained by substituting K for $y(t)$ in (2.3). for the value of cash flows occurring after u in (2.3), rewritten to a sum of fixed and floating legs. Furthermore, for modeling the forward swap rate $y(t)$, we define the process

$$y(t) = y(0) + \int_0^t \sigma(s) dW(s). \tag{2.7}$$

First we need to check that there are no arbitrage opportunities available in the framework we previously defined. In other words, the discounted price process (discounted by the numeraire $M(t)$) needs to be a martingale under the risk neutral measure $\mathbb{Q}$.

In terms of choosing the numeraire, we note that numeraires consists of a broad collection of stochastic processes. [6] (see Section 1.3.5 therein) states that positive assets (or a sum of positive assets) are a part of this collection, and we choose the numeraire as $M(t) = \text{pvbp}_{i(u)}(t)$, because the $\text{pvbp}_{i(u)}(t)$ is a sum of positive assets.

$\forall s, t$ with $0 \leq s \leq t \leq u$, u fixed, we have

$$\begin{aligned}
\mathbb{E}\left[\frac{V(t)}{M(t)}\middle|\mathscr{F}(s)\right] &= \mathbb{E}\left[\frac{N \cdot (y(t) - K) \cdot \text{pvbp}_{i(u)}(t)}{\text{pvbp}_{i(u)}(t)}\middle|\mathscr{F}(s)\right] \\
&= N \cdot \mathbb{E}\left[y(0) + \int_0^t \sigma(x) dW(x) - K\middle|\mathscr{F}(s)\right] \\
&= N \cdot \left(y(0) - K + \int_0^s \sigma(x) dW(x) + \mathbb{E}\left[\int_s^t \sigma(x) dW(x)\middle|\mathscr{F}(s)\right]\right)
\end{aligned}$$

$$
\begin{aligned}
&\overset{(a)}{=} N \cdot \left(y(0) - K + \int_0^s \sigma(x) dW(x) \right) \\
&= N \cdot \left(y(0) - K + \int_0^s \sigma(x) dW(x) \right) \cdot \frac{\text{pvbp}_{i(u)}(s)}{\text{pvbp}_{i(u)}(s)} \\
&= \frac{N \cdot (y(s) - K) \cdot \text{pvbp}_{i(u)}(s)}{\text{pvbp}_{i(u)}(s)} \\
&= \frac{V(s)}{\text{pvbp}_{i(u)}(s)} \\
&= \frac{V(s)}{M(s)}, \qquad (2.8)
\end{aligned}
$$

where in (a) the expectation is equal to zero, because we make use of the fact that a stochastic integral with respect to a Brownian motion is a martingale. We can conclude by (2.8) that our framework is arbitrage free under the risk neutral measure $\mathbb{Q}$. Now we look into the EPE in the fully collateralized case at observation date u, which is defined as

$$
\text{EPE}(u) = \mathbb{E}\left[\left(M(0) \cdot \frac{V(u)}{M(u)} - M(0) \cdot \frac{V(u-\delta)}{M(u-\delta)} \right)^+ \right]. \qquad (2.9)
$$

The formula in (2.9) describes the expected positive change of the discounted portfolio values in the period $[u - \delta, u]$. Furthermore, looking inside the brackets in (2.9), and comparing this to the definition of exposure in the fully collateralized case in formula (2.1), we note that

$$
c(u-\delta) = M(0) \cdot \frac{V(u-\delta)}{M(u-\delta)},
$$

which aligns with the assumption that the MPoR starts at the last day that the counterparty posts collateral. See for illustration Figure 2.2, where the gray dots are the discounted portfolio values at time $u - \delta$ and u for a single path. The EPE at time u is calculated by calculating the expectation of the positive changes in the discounted portfolio values in the time period $[u - \delta, u]$.

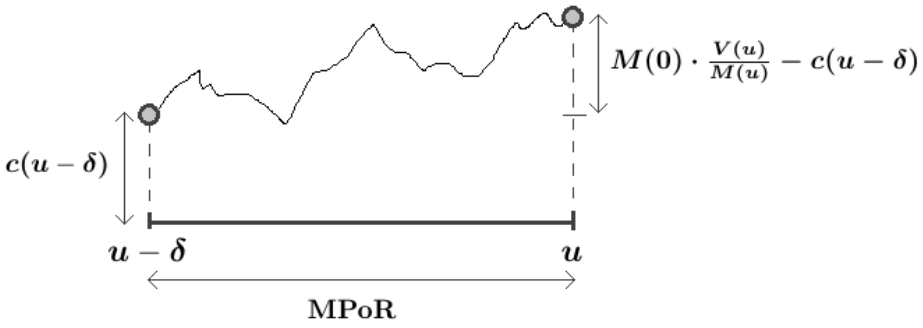

Figure 2.2: The EPE at time u is calculated as the expectation of positive changes between the discounted portfolio values in the period $[u-\delta, u]$, where these changes are shown for a single path in this figure.

Substituting the value of the swap shown in (2.3) in the formula of the EPE at time u in (2.9) gives us:

$$
\begin{aligned}
\mathrm{EPE}(u) &= \mathbb{E}\left[\left(M(0)\cdot\frac{V(u)}{M(u)} - M(0)\cdot\frac{V(u-\delta)}{M(u-\delta)}\right)^+\right] \\
&= M(0)\cdot\mathbb{E}\left[\left(\frac{V(u)}{M(u)} - \frac{V(u-\delta)}{M(u-\delta)}\right)^+\right] \\
&\overset{(a)}{=} \mathrm{pvbp}_{i(u)}(0)\cdot N\cdot\mathbb{E}\Big[(y(u)-y(u-\delta))^+\Big] \\
&= \mathrm{pvbp}_{i(u)}(0)\cdot N\cdot\mathbb{E}\left[\Big(\int_{u-\delta}^{u}\sigma(x)dW(x)\Big)^+\right] \\
&\overset{(b)}{=} \mathrm{pvbp}_{i(u)}(0)\cdot N\cdot\mathbb{E}\Big[\mathbb{1}_{\{Z^*\geq 0\}}\cdot Z^*\Big] \\
&\overset{(c)}{=} \mathrm{pvbp}_{i(u)}(0)\cdot N\cdot\mathbb{E}\left[\mathbb{1}_{\{Z\geq 0\}}\cdot\sqrt{\int_{u-\delta}^{u}\sigma^2(s)ds}\cdot Z\right] \\
&= \mathrm{pvbp}_{i(u)}(0)\cdot N\cdot\sqrt{\int_{u-\delta}^{u}\sigma^2(s)ds}\cdot\mathbb{E}[\mathbb{1}_{\{Z\geq 0\}}\cdot Z] \\
&= \mathrm{pvbp}_{i(u)}(0)\cdot N\cdot\sqrt{\int_{u-\delta}^{u}\sigma^2(s)ds}\cdot\int_0^\infty x\cdot\frac{1}{\sqrt{2\pi}}\cdot e^{-\frac{1}{2}x^2}dx \\
&\overset{(d)}{=} \mathrm{pvbp}_{i(u)}(0)\cdot N\cdot\sqrt{\int_{u-\delta}^{u}\sigma^2(s)ds}\cdot\frac{1}{\sqrt{2\pi}}\cdot\frac{\Gamma(1)}{2\cdot\frac{1}{2}}
\end{aligned}
$$

$$= \text{pvbp}_{i(u)}(0) \cdot N \cdot \sqrt{\int_{u-\delta}^{u} \sigma^2(s)ds} \cdot \frac{1}{\sqrt{2\pi}}, \tag{2.9}$$

with the following remarks:

(a) For the numeraire we choose $M(t) = \text{pvbp}_{i(u)}(t)$.

(b) $Z^* \sim \mathcal{N}(0, \int_{u-\delta}^{u} \sigma^2(s)ds)$.

(c) $Z \sim \mathcal{N}(0,1)$ and the fact that $\{Z^* \geq 0\}$ and $\{Z \geq 0\}$ are equal sets.

(d) $\int_0^\infty x^n \cdot e^{-ax^2} dx = \frac{\Gamma(\frac{n+1}{2})}{2a^{(n+1)/2}}$.

Our conclusion is that we only need to specify the volatilities $\sigma(x)$ for $x \in [u-\delta, u]$, to be able to generate values for the EPE for different observation dates u, resulting in an EPE profile. At last we will simplify the formula in (2.9), by assuming that the volatility is constant in the period $[u-\delta, u]$. This assumption comes from the fact that volatilities can be considered to be constant on small time periods. This assumption will result in the following formula for the EPE in the period $[u-\delta, u]$:

$$\text{EPE}(u) = \text{pvbp}_{i(u)}(0) \cdot N \cdot \sqrt{\delta} \cdot \sigma(u) \cdot \frac{1}{\sqrt{2\pi}}. \tag{2.10}$$

Now we take a look at (2.10) in an intuitive way. If the present value of a basis point at time 0 of fixed cash flows after observation date u, $\text{pvbp}_{i(u)}(0)$, increases, the EPE at observation date u will also increase. This is because there will be more fixed cash flows after observation date u (assuming that all accrual factors and discount factors are unchanged). Note that the EPE profile decreases over time, because there will be less upcoming fixed cash flows when we get closer to maturity T. If the notional N increases, the total underlying amount of the trade will increase, which again causes the EPE to increase. Furthermore, if the volatility at observation date u increases, there will be more uncertainty, which causes the EPE at observation date u to increase.

With the simplification of the formula of the EPE at observation date u in (2.10), we only need to estimate the volatilities $\sigma(u)$ for $u \in [0, T]$. These estimations will be obtained by the method of calibration, shown in Section 2.3.

2.3 Obtaining volatilities through calibration

To obtain the volatilities needed for equation (2.10), we will make use of calibration. The method of calibration consists of estimating the values of various parameters, by comparing results of our model in (2.10) with the results of another model, in terms of generating an EPE profile. By minimizing these differences we obtain the volatilities $\sigma(u)$ for $u \in [0, T]$. In this section we start with explaining the underlying theory of the method of calibration. We then talk about the software we use for calibration, where we specify this calibration procedure to obtain volatilities needed for our model to generate an EPE profile. At last we compare and discuss the EPE profiles generated by our model and the model used for calibration.

2.3.1 Calibration method

To obtain a calibration method, which we will use to get approximations for the volatilities needed for our model, we start with the no arbitrage condition applied to both the model used for calibration and our own model. $\hat{V}(t)$ and $\hat{M}(t)$ are respectively the swap value and the numeraire at time t of the model used for calibration, while $V(t)$ and $M(t)$ are respectively the swap value and numeraire at time t of our model. For both the model used for calibration and our model, the discounted price processes (discounted by the numeraire of the respective model) need to be a martingale under the risk neutral measure $\mathbb{Q}$. $\forall t$ with $0 \leq t \leq u$, u fixed, we have

$$\mathbb{E}\left[M(0)\frac{V(t)}{M(t)}\right] = V(0) \quad \text{and} \quad \mathbb{E}\left[\hat{M}(0)\frac{\hat{V}(t)}{\hat{M}(t)}\right] = V(0). \tag{2.11}$$

The equations in (2.11) both need to satisfy, so we get

$$\begin{aligned}
\mathbb{E}\left[\hat{M}(0)\frac{\hat{V}(t)}{\hat{M}(t)}\right] &= \mathbb{E}\left[M(0)\frac{V(t)}{M(t)}\right] \\
&\overset{(a)}{=} \mathbb{E}\left[\text{pvbp}_{i(u)}(0) \cdot \frac{(y(t) - K) \cdot \text{pvbp}_{i(u)}(t)}{\text{pvbp}_{i(u)}(t)}\right] \\
&= \mathbb{E}\Big[\text{pvbp}_{i(u)}(0) \cdot (y(t) - K)\Big] \\
&\overset{(b)}{=} \mathbb{E}\left[\hat{M}(0)\frac{\hat{V}(t)}{\hat{M}(t)}\right],
\end{aligned}$$

with the following remarks:

(a) For the numeraire we choose $M(t) = \text{pvbp}_{i(u)}(t)$.

(b) Here we made the substitution

$$\hat{y}(t) = \frac{\hat{M}_l(0)\frac{\hat{V}_l(t)}{\hat{M}_l(t)}}{\text{pvbp}_{i(u)}(0)} + K, \tag{2.12}$$

which will be an approximation for the forward swap rate $y(t)$ in (2.7).

By calculating the volatility of the variable $\hat{y}(t)$ in (b), we obtain an estimation for the volatility of the forward swap rate at time t, which we need to obtain values for the EPE in (2.10). In the next section we will explain how to obtain the volatilities for $\hat{y}(u)$, $u \in [0, T]$, by making use of openly available software.

2.3.2 Calibration with open source software

We make use of open source software called *Open Source Risk Engine*[1] (ORE), which is based on Quantlib[2] (open source library for quantitative finance). ORE has been initially released by Quaternion Risk management on 7 October 2016, and currently provides portfolio pricing, cash flow generation, sensitivity analysis, stress testing, and a range of contemporary derivative portfolio analytics. The latter is based on a crude Monte Carlo simulation framework that produces certain market risk measures as expected positive exposure, which are relevant for our framework.

Furthermore, ORE provides 23 example codes, which gives a number of standard reports and exposure graphs as output. We will make use of example code 10 specifically, which is able to generate an EPE profile in the case of a portfolio with collateralization (exposures are fully collateralized). For the EPE profile, ORE uses discounted portfolio values that are obtained by simulation. We will modify this example code to be aligned with our setting of having a portfolio with one fixed versus floating interest rate swap. To have a detailed description of ORE, see the user-guide [7].

In the framework of ORE (example code 10), we assumed we perform our calculations at a valuation date, which is chosen to be 5-Feb-2016. The trade portfolio consists of one 1Y fixed (pay) vs 3M floating (receive) interest rate

[1] `http://www.opensourcerisk.org/`

[2] `https://www.quantlib.org/`

swap with start date 5-May-2016 (date of first cash flow), maturity date 6-Feb-2021, $T = 5$Y, notional N=100, fixed rate K=0.01, while for the MPoR we chose a duration of ten days, which corresponds to $\delta = 10$.

See Figure 2.3 for an illustration of the swap. For all specific details in terms of simulation with ORE, see Appendix B.

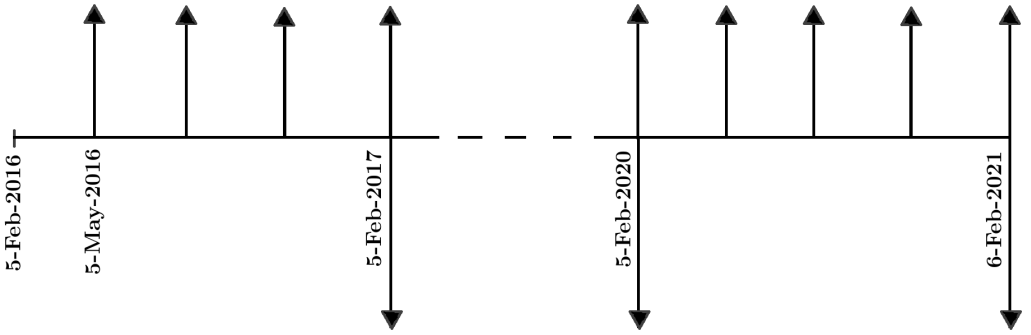

Figure 2.3: Illustration of a 1Y fixed (pay) vs 3M floating (receive) interest rate swap where the first cash flow occurs on 5-May-2016, and where the last cash flows occurs on 6-Feb-2021. We assume that CVA calculations are made on 5-Feb-2016.

The calibration procedure goes as follows:

(1) For every path l, where $l \in \{1, \ldots, L\}$, and for every grid point u, simulate discounted portfolio values $\hat{M}_l(0)\frac{\hat{V}_l(u)}{\hat{M}_l(u)}$.

(2) For every path l and every grid point u, calculate approximations for the forward swap rate at time u, described in (2.12).

(3) For every grid point u, calculate the approximation of the volatility of the forward swap rate, $\hat{\sigma}(u)$. This is the volatility of the approximations of the forward swap rate at all paths at grid point u, obtained in (2).

By performing the calibration procedure, we are able to calculate expected positive exposures for every grid point u, by substituting the approximations of the volatility of the forward swap rate at observation date u in equation (2.10), resulting in an EPE profile.

Furthermore, in terms of calibration, ORE makes use of swaptions to calibrate their interest rate models. A swaption is a financial product that grants its owner the right but not the obligation to enter into an underlying

swap. According to [4] (see Section 3.4.1 therein), we can note that in our framework, where we have a portfolio consisting of one interest rate swap, the volatilities of the forward swap rates of the interest rate swap (which are the volatilities we needed to approximate in (2.10)) are equal to the volatilities of the forward swap rates of these swaptions. The reason why we do not obtain the volatilities of our forward swap rate this way is because ORE does not give these volatilities as output, and it is unknown what interpolation method ORE uses between these volatilities, to obtain volatilities for every observation date u, which we need in order to generate an EPE profile with (2.10).

In Figure 2.4 we show the EPE profiles generated by ORE and our model, for the swap described earlier. Furthermore, ORE makes the following assumptions about cash flows during the MPoR:

(1) During the MPoR, the bank makes payments towards the failing counterparty.

(2) During the MPoR, the failing counterparty makes payments towards the bank.

We assumed in our framework that no cash flows are present during the MPoR, so we do not take assumptions (1) and (2) into account, as this does not always reflect common market practice in financial situations.

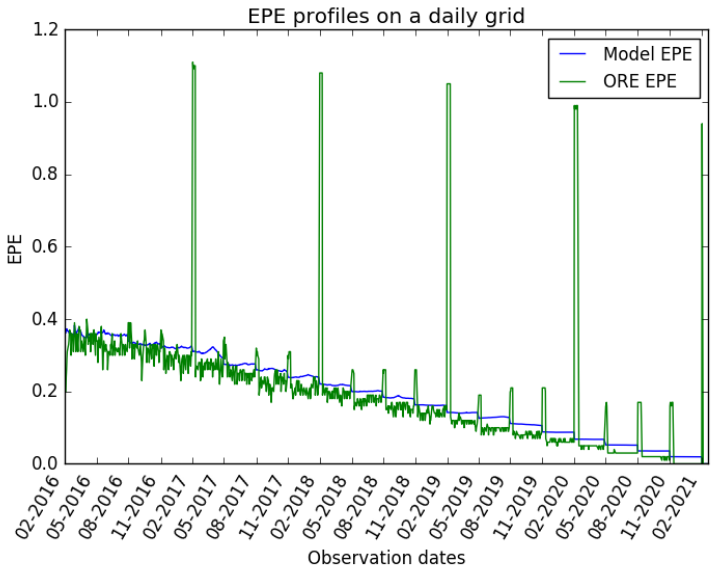

Figure 2.4: Graph of the EPE profiles generated by ORE and our model. Simulation with 300 paths on a daily grid.

The assumptions (1) and (2) that ORE makes about cash flows, are the reasons for the spikes seen in Figure 2.4. In the interest rate swap we considered, the bank pays a fixed cash flow towards the counterparty on a yearly basis, while on a quarterly basis, the bank receives a floating cash flow from the counterparty. Looking again at assumptions (1) and (2) that ORE makes, it would be intuitive to expect the spikes at the floating cash flow dates in Figure 2.4 to be facing downwards, because at these dates the bank receives payments from the counterparty.

Unfortunately we are unable to explain the spikes that occur caused by the floating cash flows, but we will now explain that these spikes (caused by fixed and floating cash flows) do not have a significant impact, in terms of the calculation of CVA.

When we are computing the CVA of this portfolio, we are basically calculating an integral in (1.3) or a summation in (1.4). The spikes occur on a quarterly basis, and cause an increase of the EPE at a small amount of observation dates u, compared to the total amount of observation dates. Thus, we can conclude that the spikes only make a small difference for the value of the CVA of this portfolio.

Note that the EPE of our model is larger than the EPE of ORE at observation dates u, except when there is a payment present in $[u - \delta, u]$. One of the reasons is the following: when we discretize with a certain grid

(in our case we discretized with a daily grid), the EPE of ORE is calculated as

$$\widehat{\mathrm{EPE}}(u) = \mathbb{E}\left[\left(\hat{M}(0)\cdot\frac{\hat{V}(u)}{\hat{M}(u)} - \hat{M}(0)\cdot\frac{\hat{V}(u-\delta)}{\hat{M}(u-\delta)}\right)^{+}\right], \tag{2.13}$$

where $\hat{M}(x)$ is the value of the numeraire that ORE uses at time x, and where u is a grid point (observation date) used to calculate the EPE at that time. If $u-\delta$ is not a point on that grid, ORE will instead use the closest grid point available, which will either be the grid point on the left at time a, or the grid point on the right at time b, according to the illustration shown in Figure 2.5. ORE uses the grid point b instead of $u-\delta$, to calculate the EPE at time u.

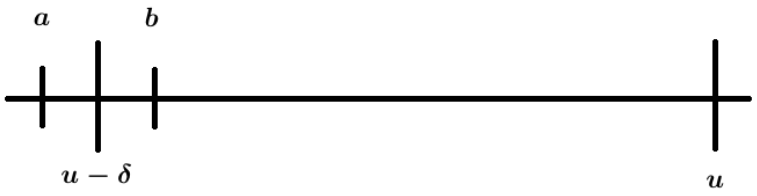

Figure 2.5: For obtaining the EPE at time u in (2.13), if $u-\delta$ is not a grid point, ORE calculates the EPE for the interval $[b,u]$ instead for the interval $[u-\delta,u]$, resulting in a MPoR of less than δ days.

This will result in a lower EPE profile, in the case for ORE, because the duration of the MPoR, δ, is reduced at times where $u-\delta$ is not a grid point. Now we increase the time step size of the grid to weekly instead of daily. See Figure 2.6 where the EPE profiles of both our model and ORE are shown:

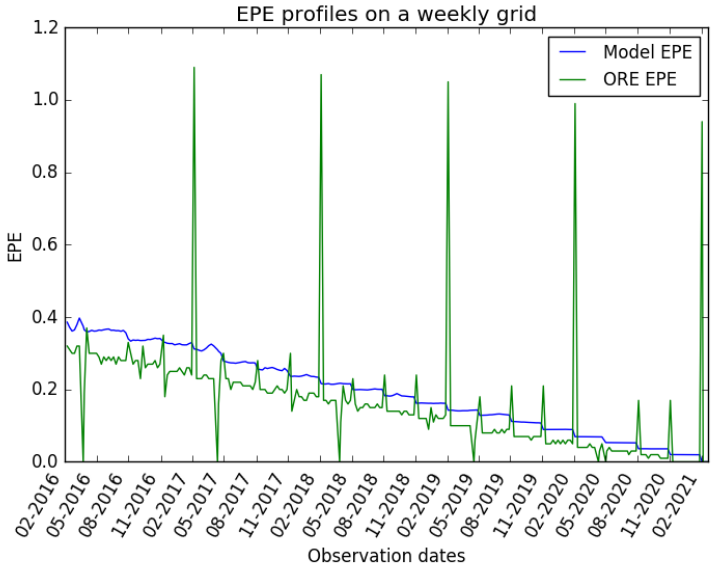

Figure 2.6: Graph of the EPE profiles generated by ORE and our model. Simulation with 300 paths on a weekly grid.

Note that the difference between our model and the model from ORE is larger compared to the difference between these models displayed in Figure 2.4. This happens because when we use weekly time steps and an MPoR of ten days ($\delta = 10$), ORE actually calculates a EPE corresponding to a MPoR of fewer days (seven to be precise), because $u - \delta$ is not a grid point, and ORE chooses the data from an observation date closer to u instead. This means that the MPoR duration is decreased, which results in a lower EPE profile.

Also note the presence of spikes facing downward from the model of ORE in Figure 2.6. These spikes occur when the period between observation dates is larger than ten days (this can be caused by calendar vacation dates and weekends), which causes ORE to use the same observation date in (2.13), resulting in the EPE being equal to zero at time u (which is incorrect).

In the case of generating an EPE profile with ORE, we note that, we still need to simulate discounted portfolio values $\hat{M}(0)\frac{\hat{V}(u)}{\hat{M}(u)}$ for observation dates u on a daily grid. When simulation is done on a grid larger that daily, ORE generates less accurate EPE profiles, as seen between Figures 2.4 and 2.6. Furthermore, daily simulation can be computationally infeasible, when we deal with large portfolios and long time horizons. In Section 2.4, we introduce a method where we can obtain EPE profiles on a daily grid, while only

simulating discounted portfolio values on a grid where the time step size is larger than daily (weekly, biweekly, monthly, quarterly, etc.).

2.4 The Brownian bridge method

The Brownian bridge method allows us to avoid brute-force daily simulation of discounted portfolio values, by constructing a Brownian bridge between two points on a grid where the time step size are larger than daily. This can be useful when we deal with large portfolios, where having to calculate portfolio values on a daily basis can be computationally infeasible. Furthermore, some applications can only calculate discounted portfolio values on a pre-specified grid, and implementing a method like this gives the option to obtain approximations of portfolio values on a daily grid. We mainly follow the method described in [5] (see Section 8.2 therein), which we will adjust to our own setting.

We start by formulating the steps that are involved in the (standard) Brownian bridge method:

(Standard) Brownian bridge method

(1) For each path l, $l \in \{1, \ldots, L\}$, and every portfolio valuation point s_j, $j \in \{1, \ldots, J\}$ (time step size of the grid should be larger than daily), simulate the discounted portfolio values, $\hat{M}_l(0)\frac{\hat{V}_l(s_j)}{\hat{M}_l(s_j)}$.

(2) For every grid point u, compute the local variance $\sigma^2(s_j, s_{j+1})$ for the portfolio "diffusion" between s_j and s_{j+1},

$$\hat{M}_l(0)\frac{\hat{V}_l(s_{j+1})}{\hat{M}_l(s_{j+1})} - \hat{M}_l(0)\frac{\hat{V}_l(s_j)}{\hat{M}_l(s_j)}, \qquad \forall l \in \{1, \ldots, L\},\ j = 1, \ldots, J-1,$$

via a kernel density estimator. According to [8] (see Section 2 therein), the kernel density estimation of a density f at the point x is given by

$$\hat{f}_{h,[s_j,s_{j+1}]}(x) = \frac{1}{L \cdot h} \sum_{l=1}^{L} Ker\left(\frac{x - X_l}{h}\right),$$

where in our case, we have that

$$X_l = \hat{M}_l(0)\frac{\hat{V}_l(s_{j+1})}{\hat{M}_l(s_{j+1})} - \hat{M}_l(0)\frac{\hat{V}_l(s_j)}{\hat{M}_l(s_j)},$$

as random variables with density f. Ker is the kernel function that satisfies the conditions

$$\int_{-\infty}^{\infty} Ker(x)dx = 1,$$

and

$$Ker(-x) = Ker(x) \quad \forall x,$$

which are the normalization and symmetry conditions respectively. Furthermore, h is a smoothing parameter known as the bandwidth. We will make use of the Gaussian kernel, which means that for Ker, we have

$$Ker(y) = \frac{1}{\sqrt{2\pi}} \cdot \exp\left(-\frac{y^2}{2} \right).$$

For our selection of bandwidth h, we use Silverman's rule of thumb in [8] (see Section 3.1 therein), where for h, we choose

$$h = \left(\frac{4}{3} \cdot \frac{\hat{\sigma}^5}{L} \right)^{\frac{1}{5}},$$

with $\hat{\sigma}$ being the standard deviation of the samples X_i [3].

(3) For each path l and each grid point s_j, simulate an independent, daily sampled, Brownian bridge process (see Section 3.1 in [10]) that starts with the value $\hat{M}_l(0)\frac{\hat{V}_l(s_j)}{\hat{M}_l(s_j)}$ at time s_j, and ends at $\hat{M}_l(0)\frac{\hat{V}_l(s_{j+1})}{\hat{M}_l(s_{j+1})}$ at time s_{j+1}. For the Brownian motion $B_l(u)$, where $s_j < u < s_{j+1}$, we have that $B(u)$ is normally distributed with conditional mean

$$\begin{aligned} \mathbb{E}[B_l(u)|B_l(s_j) = x, B_l(s_{j+1}) = y] &= \frac{(s_{j+1} - u) \cdot x + (u - s_j) \cdot y}{s_{j+1} - s_j} \\ &= x + (y - x) \cdot \frac{u - s_j}{s_{j+1} - s_j}, \end{aligned} \tag{2.14}$$

[3] In [5] (see p35 therein) it is stated that there is another method available to obtain the local variance, by making use of the Nadaraya-Watson Gaussian kernel regression estimator, which is described in [9] (see p141-142 therein).

and conditional variance

$$\mathrm{Var}[B_l(u)|B_l(s_j) = x, B_l(s_{j+1}) = y] = \sigma^2(s_j, s_{j+1}) \cdot \frac{(s_{j+1} - u) \cdot (u - s_j)}{s_{j+1} - s_j}. \tag{2.15}$$

(4) For each path l and each portfolio valuation point s_j, the portfolio values for every grid point u, with $s_j < u < s_{j+1}$, are approximated by the simulated Brownian bridge point $B_l(u)$:

$$\hat{M}_l(0)\frac{\hat{V}_l(u)}{\hat{M}_l(u)} \approx B_l(u). \tag{2.16}$$

Furthermore, according to [10] (see Section 3.1 therein), if we assume we have determined the values $B(u_1) = x_1, B(u_2) = x_2, \ldots, B(u_k) = x_k$ at times $s_j < u_1 < u_2 < \ldots < u_k < s_{j+1}$, and that we wish to sample $B(u_{k+1})$, with $u_k < u_{k+1} < s_{j+1}$, then

$$\begin{aligned}&(B(u_{k+1})|B(s_j) = x, B(s_{j+1}) = y, B(u_j) = x_j, j = 1, \ldots, k)\\ &= (B(u_{k+1})|B(u_k) = x_k, B(s_{j+1}) = y).\end{aligned} \tag{2.17}$$

Equality (2.17) tells us that both conditional distributions are the same, which means that conditioning on all $B(u_k)$, $B(s_j)$ and (B_{j+1}), is the same as conditioning on the two points closest to $B(u_{k+1})$, which are $B(u_k)$ and $B(s_{j+1})$. The same conclusion can be derived from the Markov Property of Brownian motion, described in [11] (see Section 2.1, Proposition 2.3(iv)). We can conclude that

$$\begin{aligned}&(B(u_{k+1})|B(s_j) = x, B(s_{j+1}) = y, B(u_j) = x_j, j = 1, \ldots, k)\\ &\sim N\left(x_k + (y - x_k) \cdot \frac{u_{k+1} - u_k}{s_{j+1} - u_k}\ ,\ \sigma^2(s_j, s_{j+1}) \cdot \frac{(s_{j+1} - u_{k+1}) \cdot (u_{k+1} - u_k)}{s_{j+1} - u_k}\right),\end{aligned}$$

which tells us that when constructing a point in the Brownian bridge, we only have to look at the values of the two points nearest to that point.

See an example of the construction of a point in the Brownian bridge in Figure 2.7, where the value at time u is normally distributed, with (2.14) and (2.15) as conditional mean and conditional variance, respectively.

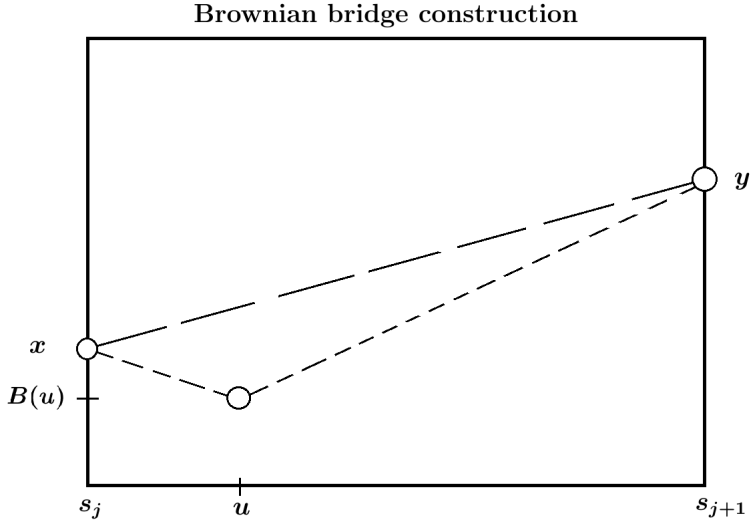

Figure 2.7: Example of the construction of a point u in the Brownian bridge, between the portfolio valuation points s_j and s_{j+1}.

In step (1) in the Brownian bridge method, we again make use of the simulated discounted portfolio values obtained by ORE, with the same fixed (pay) versus floating (receive) interest rate swap described in Section 2.2. We will simulate the discounted portfolio values on a daily grid, and obtain the simulated discounted portfolio values at every portfolio simulation point s_j, for every path. We then build Brownian bridges between these portfolio valuation points, with steps (2), (3) and (4) in the Brownian bridge method.

Note that we do not make use of the simulated discounted portfolio values of ORE, simulated on portfolio valuation points s_j, where the time step size is larger than daily, and build Brownian bridges between those portfolio valuation points. Instead we simulate the discounted portfolio values on a daily grid (with ORE), where we then take portfolio valuation points to be on a larger grid, and then build Brownian bridges between these chosen portfolio valuation points. With this approach we can exactly compare the performance of daily simulation against simulating on a larger grid and obtaining discounted portfolio values on a daily grid with the Brownian bridge method.

By applying the Brownian bridge method, we obtain discounted portfolio values, $\hat{M}_l(0)\frac{\hat{V}_l(u)}{\hat{M}_l(u)}$, for every path l and every daily grid point u. We are now able to generate an EPE profile with the discounted portfolio values obtained by the Brownian bridge method.

Note that in the Brownian bridge method, in order to have accurate results, we need to have approximations of the conditional mean and conditional variance shown in (2.14) and (2.15) that are close to the real conditional expectation and conditional variance (from the discounted portfolio values simulated on a daily grid by ORE), for every observation date. When we apply the Brownian bridge method between two portfolio valuation points, in the case of a cash flow occurring between these portfolio valuation points, the conditional expectation and conditional variance are not correctly estimated (which we will show and explain later in this section). To deal with this problem, we introduce a second method, which we refer to as the new Brownian bridge method:

New Brownian bridge method

(1) Take the valuation date (the date when the CVA calculations are being made) of the simulation process, and every cash flow date as portfolio valuation dates s_j.

(2) For every portfolio valuation date s_j, the nearest observation dates to the left and right side of s_j, will be added as new portfolio valuation dates, referred to as s_j^{left} and s_j^{right}.

(3) The Brownian bridge method is applied between portfolio valuation dates s_j^{right} and s_{j+1}^{left}, as seen in Figure 2.8 (s_j^{right} and s_{j+1}^{left} are shown as white dots), where the arrows facing upwards are floating cash flows the bank receives from the counterparty, and where the arrows facing downward are fixed cash flows the bank pays to the counterparty. At the valuation date, when there is no payment yet, we can build the Brownian bridge starting at the first portfolio valuation point s_1 and ending at s_2^{left}.

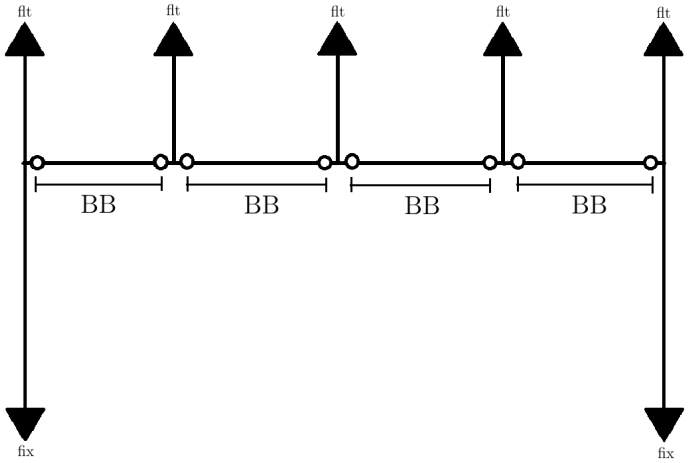

Figure 2.8: By building the Brownian bridges between points where cash flow dates are not occurring in, we avoid the disruption caused by these cash flows, in terms of estimating the conditional expectation and conditional variance in (2.14) and (2.15), for every observation date.

Now we show some graphs of EPE profiles, obtained by ORE and by different Brownian bridge methods. We start with the case of applying both Brownian bridge methods on monthly time steps, with 300 and 1000 paths, shown in Figures 2.9 and 2.10, respectively:

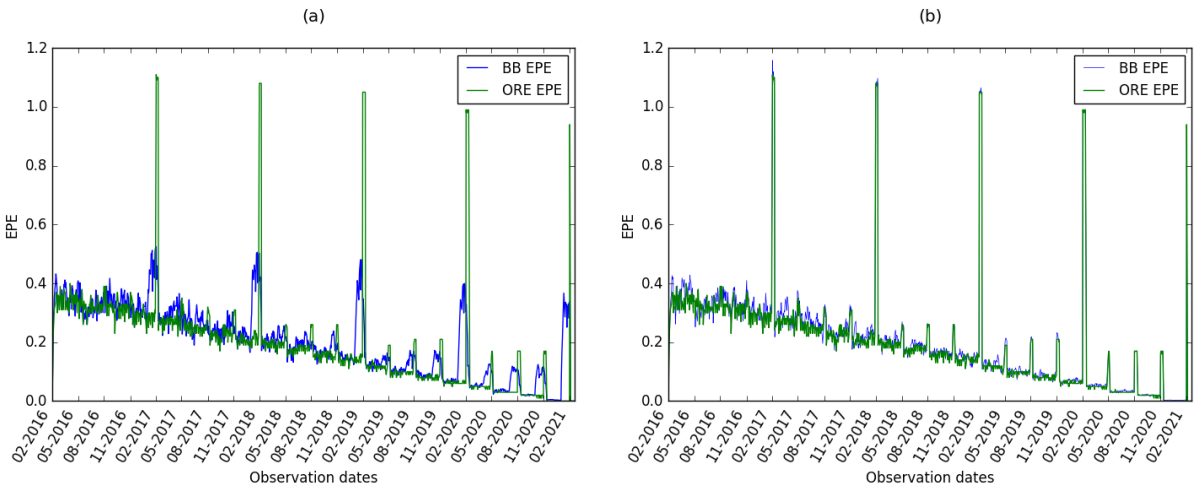

Figure 2.9: Graphs of EPE profiles generated by ORE and the Brownian bridge method. Simulation with 300 paths on a daily grid. With the Brownian bridge method, we used monthly time steps, where we constructed, per path, a Brownian bridge between every portfolio valuation point s_j. In graph **(a)**, the standard Brownian bridge method is applied, with the portfolio valuation points chosen to be cash flow dates. In graph **(b)**, we applied the new Brownian bridge method .

We can see in graph **(a)** in Figure 2.9 that the EPE profile generated with the standard Brownian bridge method is inaccurate. Especially at the cash flow dates, where in the EPE profile generated by ORE spikes upwards occur. The standard Brownian bridge method is unable to correctly capture these spikes, because of the cash flow(s) occurring between or at the portfolio valuation points, which causes the conditional mean and conditional expectation shown in (2.14) and (2.15) to be incorrectly estimated for every observation date. In graph **(b)** in Figure 2.9, we see the EPE profile generated by the new Brownian bridge method, which succeeds in accurately estimating the conditional mean and conditional variance shown in (2.14) and (2.15). We obtain accurate results because the new Brownian bridge method is not applied in time periods where cash flows occur, and the discounted portfolio values at these cash flow dates are obtained by simulation with ORE. Now lets take a look what happens when we increase the number of paths in our simulation:

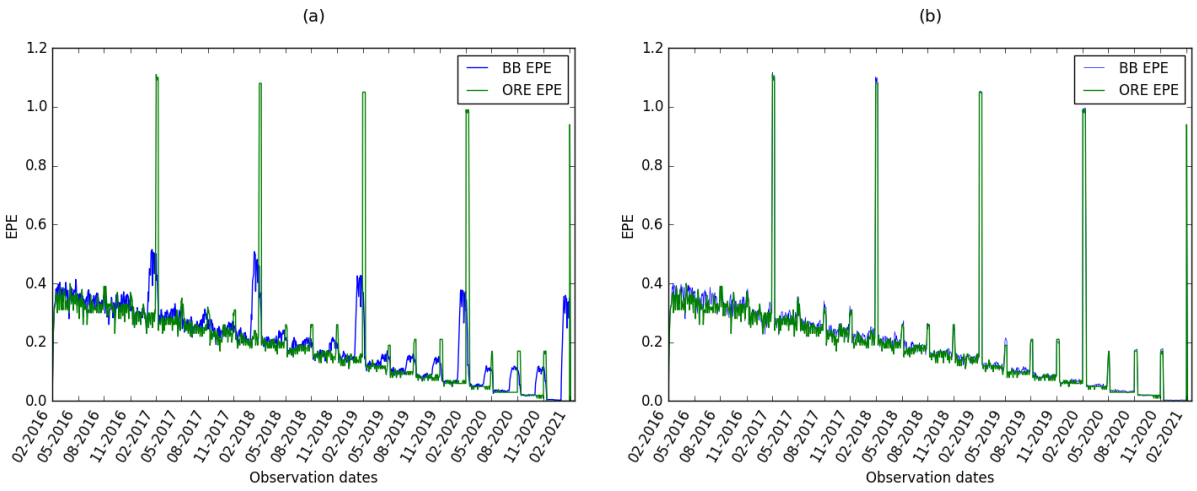

Figure 2.10: Graphs of EPE profiles generated by ORE and the Brownian bridge method. Simulation with 1000 paths on a daily grid. With the Brownian bridge method, we used monthly time steps, where we constructed, per path, a Brownian bridge between every portfolio valuation point s_j. In graph **(a)**, the standard Brownian bridge method is applied, with the portfolio valuation points chosen to be cash flow dates. In graph **(b)**, we applied the new Brownian bridge method .

We can see that in graph **(a)** in Figure 2.10, the standard Brownian bridge method still fails to accurately estimate the EPE profile, even when the amount of paths is increased. In graph **(b)** in Figure 2.10, we can see that the EPE profile generated by the new Brownian bridge method is a bit more accurate when the amount of paths is increased (compared to graph **(b)** in Figure 2.9), especially in the time period between February 2016 and February 2018.

In Table 2.1, the mean squared errors (MSE) are calculated, where we compared the EPE profile of ORE with both EPE profiles obtained by making use of the standard and the new Brownian bridge method: the mean squared errors are calculated for both the standard and new Brownian bridge method.

MSE		Number of paths		
		300	1000	2000
Method	Standard	0.01889	0.01889	0.01871
	New	0.00044	0.00026	0.00020

Table 2.1: Table where the mean squared error is calculated, between the standard and new Brownian bridge method, with different number of paths.

We can conclude, by looking at the graphs of the EPE profiles in Figures 2.9 and 2.10, and the mean squared errors in Table 2.1, that the new Brownian bridge method is better than the standard Brownian bridge method in terms of creating an accurate EPE profile with monthly time steps.

In our framework, we consider a portfolio of a single interest rate swap where cash flows occur on a quarterly basis, so we can take a look at what happens if we increase the time step size from monthly to quarterly. Figures 2.11 and 2.12 show EPE profiles generated by ORE and both Brownian bridge methods (where cash flow dates are chosen as portfolio valuation points), in the setting of quarterly time steps, with 300 and 1000 paths respectively:

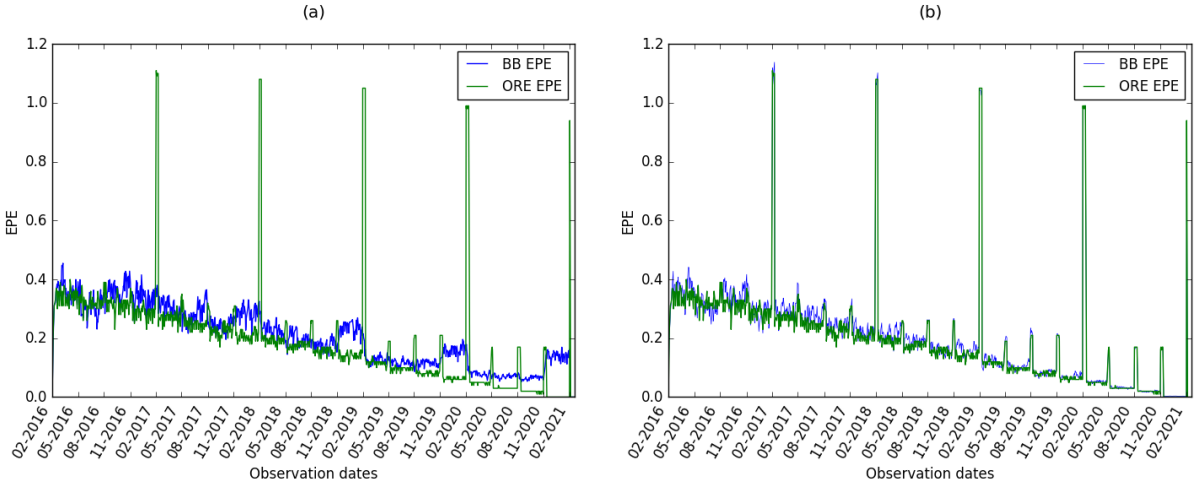

Figure 2.11: Graphs of EPE profiles generated by ORE and the Brownian bridge method. Simulation with 300 paths on a daily grid. With the Brownian bridge method, we used quarterly time steps, where we constructed, per path, a Brownian bridge between every portfolio valuation point s_j. In graph **(a)**, the standard Brownian bridge method is applied, with the portfolio valuation points chosen to be cash flow dates. In graph **(b)**, we applied the new Brownian bridge method .

We can see in graph **(a)** in Figure 2.11, that the EPE profile generated by the standard Brownian bridge method is inaccurate. Again, the cash flows occurring at or between the portfolio valuation points prevent the standard Brownian bridge method to correctly estimate the conditional mean and conditional variance shown in (2.14) and (2.15). Looking at graph **(b)** in Figure 2.11, the EPE profile generated by the new Brownian bridge method succeeds in accurately approximating the EPE profile generated by ORE. Now lets take a look at what happens if we increase the number of paths in our simulation:

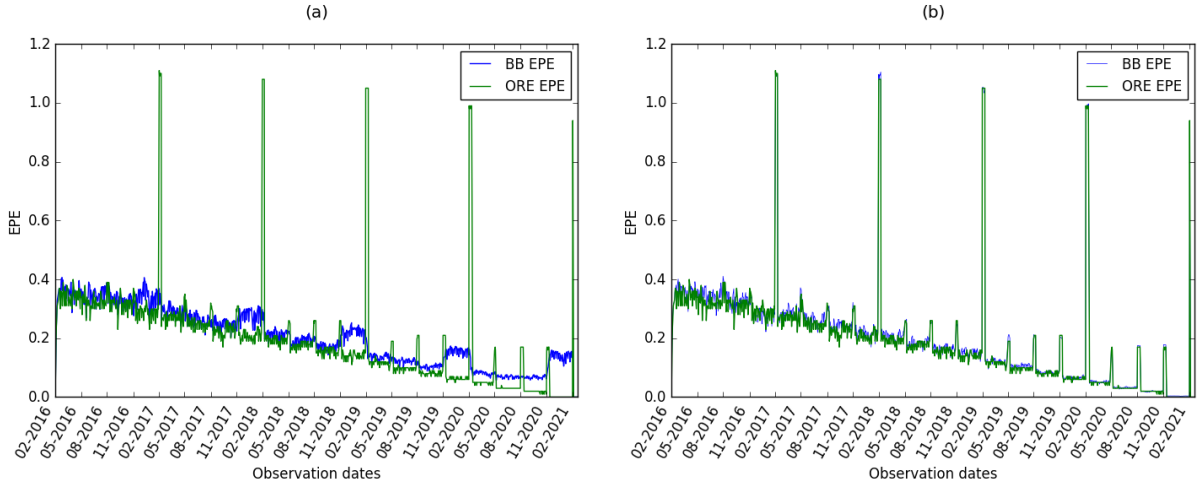

Figure 2.12: Graphs of EPE profiles generated by ORE and the Brownian bridge method. Simulation with 1000 paths on a daily grid. With the Brownian bridge method, we used quarterly time steps, where we constructed, per path, a Brownian bridge between every portfolio valuation point s_j. In graph **(a)**, the standard Brownian bridge method is applied, with the portfolio valuation points chosen to be cash flow dates. In graph **(b)**, we applied the new Brownian bridge method .

We can see that in graph **(a)** in Figure 2.12, the standard Brownian bridge method still fails to accurately estimate the EPE profile, even when the amount of paths is increased. In graph **(b)** in Figure 2.12, we can see that the EPE profile generated by the new Brownian bridge method is a bit more accurate when the amount of paths is increased (compared to graph **(b)** in Figure 2.11), especially in the time period between February 2016 and February 2018.

In Table 2.2, the mean squared errors are calculated, where we compared the EPE profile of ORE with both EPE profiles obtained by making use of the standard and the new Brownian bridge method.

MSE		Number of paths		
		300	1000	2000
Method	Standard	0.01969	0.01943	0.01936
	New	0.00058	0.00029	0.00024

Table 2.2: Table where the mean squared error is calculated, between different choices of portfolio valuation points and between what points the Brownian bridge method is applied, with different number of paths.

We can conclude, by looking at the EPE profiles in Figure 2.11 and 2.12, and the mean squared errors in Table 2.2, that the new Brownian bridge method performs better compared to the standard Brownian bridge method in terms of creating an accurate EPE profile with quarterly time steps.

Note that in our case, where cash flows occur on a quarterly basis, we are unable to apply the new Brownian bridge method on a grid larger than quarterly. The reason behind this is because we cannot avoid cash flow dates being between the portfolio valuation points where we apply the Brownian bridge method to, when the grid is larger than quarterly. The Brownian bridge method described in [5] (see Section 8.2 therein), does allow us to increase the grid to be larger than quarterly, without losing accuracy in the EPE profile. Unfortunately, we are unable to follow this method, because ORE makes use of a numeraire (the *Linear Gauss Markov* numeraire, described in [12] (see Section 11 therein)) where we are unable to obtain its values at every observation date u, which we need to perform the Brownian bridge method described in the article.

Chapter 3

CVA with Least Squares Monte Carlo

In Chapter 2 we have outlined how to generate EPE profiles by making use of discounted portfolio values obtained by crude Monte Carlo simulation. This means that the discounted portfolio values are directly simulated for each path and every time step in the simulation. Furthermore, we have described how discounted portfolio values can be generated using crude Monte Carlo simulation on a less granular grid, before being on a finer grid, by using the Brownian bridge method.

Another method to obtain (approximated) discounted portfolio values is to use the *Least Squares Monte Carlo* (LSMC) method introduced in [13], where the LSMC method is used to price American options. In our setting of making calculations for CVA, we follow the approach outlined in [3] to obtain approximations for the discounted portfolio values for each path and every time step, which we need to be able to generate EPE profiles. Some portfolios contain products that cannot be valued analytically at each simulation step, and the standard market practice is to approximate the discounted portfolio values by making use of regression functions from the LSMC method. We start with explaining the LSMC method in the setting of the framework we are going to work in, which will be a Black-Scholes setting where we have a portfolio consisting of one European call option. Then we are going to generate EPE profiles in both the uncollateralized and the fully collateralized case, where results will be shown and analyzed. On top of the notation already introduced in Chapters 1 and 2, we define the following symbols and abbreviations:

ITM	In-the-money;
r	Annual interest rate, assumed to be constant;

t_0	Valuation date;
T	Time of expiry of the European call option;
$S(t)$	Value of the underlying stock at time t ($t \in [t_0, T]$);
σ	Volatility, assumed to be constant;
K	Strike price of the European call option;
$\Phi(x)$	Standard normal cumulative distribution function at x;
$f_t(x)$	Regression function at time t, with x as input variable;
U_t	Cash flow of the European call option occurring at time T, discounted back to time t;
$\mathrm{CF}(l;t)$	Cash flow at time t at path l;
$\mathrm{LN}(\mu, \sigma^2)$	Log-normal density where μ and σ are the mean and standard deviation of the log of the log-normal density respectively.

3.1 The LSMC method

In this section we start with defining the LSMC method in a Black-Scholes setting where a portfolio containing one European call option is considered. Then, the framework where we are going to work in is explained in detail.

3.1.1 Methodology

Assume that we have N time steps in our simulation, which means that our time discretization consists of the points $t_0 := 0, t_1, \ldots, t_N := T$. We assume that we have L simulation paths. The aim of the LSMC method is to obtain approximations of discounted portfolio values at every path, at every time step. The method starts at time t_N, and works backwards over every time step until time t_0[1]. Furthermore, we introduce two approaches in terms of implementing the LSMC method, where the differences between these two approaches are in the points taken into account in the regression.

In the first approach, we only take the in-the-money (ITM) paths into account in the regression, which is referred to as the *LSMC method (ITM paths case)*. For the second approach, all paths are taken into account in the regression, which is referred to as the *LSMC method (all paths case)*. The LSMC method for a portfolio consisting of one European call option consists of the following steps, where the distinction between the first and second approach is made in step (2):

[1]We follow the LSMC method outlined in [3], but in general the simulation can start at t_0 and end at t_N.

LSMC method

At time $k = t_N, t_{N-1}, \ldots, t_0$:

(1) Calculate for every path l (where $l \in \{1, \ldots, L\}$) the intrinsic value of the European call option at time k, defined as

$$(S_k(l) - K)^+.$$

(2) Save the paths l where the values obtained in step (1) are
(a) ITM (the paths where $[(S_k(l) - K)^+ > 0]$);
(b) all paths (the paths where $[(S_k(l) - K)^+ \geq 0]$).

(3) Define X_k as the collection of stock values at time k, at the paths l obtained in step (2).

(4) Define U_k as the cash flow of the European call option occurring at time t_N, discounted to time k, at the paths l obtained in step (3).

(5) Use the *Ordinary Least Squares* (OLS) method with a regression function, where U_k is the vector of response variables and X_k is the vector of regressor variables, to determine the coefficients of the regression function.

(6) Fill in the values of the underlying stock for all paths, at time k, in the regression function in step (5). These values are discounted relative to the numeraire back to time t_0, which will be estimations of the discounted portfolio values for all paths at time k.

In the next section we are going to introduce the framework we are going to work in, where both approaches in the LSMC method are going to be implemented.

3.1.2 Framework

We choose to work in a simple Black-Scholes setting, where we consider a portfolio with one European call option. The European call option is issued at time $t_0 = 0$, expires at $T = 5$ and has K as strike price. Furthermore, the starting value of underlying stock is $S_0 = 5$, the volatility of the underlying stock is $\sigma = 0.25$ and for the annual interest rate we set $r = 0$. The underlying stock follows a *geometric Brownian motion*, which has the following stochastic differential equation:

$$dS(t) = rS(t)dt + \sigma S(t)dW(t),$$

with the analytic solution

$$S(t) = S(0) \cdot e^{(r-\frac{\sigma^2}{2})t+\sigma W(t)}.$$

Furthermore, the value at time t of a European call option for a stock that does not pay dividends is given as

$$V(t) = \Phi(d_1) \cdot S(t) - \Phi(d_2) \cdot K \cdot e^{-r(T-t)}, \tag{3.1}$$

with

$$\begin{aligned}
\Phi(x) &= \frac{1}{\sqrt{2\pi}} \int_{-\infty}^{x} e^{-\frac{t^2}{2}} dt \\
d_1 &= \frac{1}{\sigma\sqrt{T-t}} \cdot \left[\log\left(\frac{S(t)}{K}\right) + \left(r + \frac{\sigma^2}{2}\right)(T-t) \right] \\
d_2 &= d_1 - \sigma\sqrt{T-t}.
\end{aligned}$$

In terms of simulation, we use a grid that starts at $t_0 = 0$, and ends at time $T = 5$. The time step size is chosen to be 0.1, which is chosen to be equal to the duration of the MPoR [2]. Furthermore, we consider $N = 50$ time steps and $L = 10000$ paths. We do not make use of real calendar days, because we want to keep the framework simple and straightforward.

In Section 3.2 we are going to implement the LSMC method with the framework just defined, to obtain EPE profiles for both the uncollateralized and the fully collateralized case.

3.2 Obtaining EPE profiles with the LSMC method

In this section we aim to generate EPE profiles in the presence of the MPoR, where the discounted portfolio values are approximated by the LSMC method. We start with generating EPE profiles by the LSMC method in the uncollateralized case, to see how well the discounted portfolio values are approximated by the LSMC method. These EPE profiles are compared with the EPE profiles obtained with the Black-Scholes model, where the discounted

[2]Note that during the simulation, the duration of the MPoR does not matter, only the presence of the MPoR during the simulation does. δ is chosen to be equal to 0.1 for convenience sake.

portfolio values are calculated with (3.1).

3.2.1 Uncollateralized case

We use the following approximation of the EPE at time t in the uncollateralized case:

$$\begin{aligned} \mathrm{EPE}(t) &\overset{\text{(a)}}{=} \mathbb{E}\left[\left(M(0)\frac{V(t)}{M(t)}\right)^{+}\right] \\ &\overset{\text{(b)}}{\approx} \mathbb{E}\left[M(0)\frac{1}{M(t)}\cdot(f_t)^{+}\right], \end{aligned}$$

with the following remarks:

(a) The formula for the EPE at time t in the uncollateralized case has been stated in (1.2). Furthermore, we assumed that $r = 0$, so the numeraire can be left out.

(b) The value of the portfolio at time t, at every path l, is approximated by the regression function f_t.

The regression function is chosen to be a second order polynomial, i.e.,

$$f_t(x) = a(t) + b(t)\cdot x + c(t)\cdot x^2, \tag{3.2}$$

with $a(t), b(t), c(t) \in \mathbb{R}$. Working backwards over each time step, the regression coefficients at every time t are determined by minimizing

$$\sum_{l\in\Omega_{\mathrm{a}}(t)} [f_t(x(l)) - U_t(l)]^2,$$

where the input variables in the regression function are based on the paths chosen per regression step. $\Omega_{\mathrm{a}}(t)$ is either the subset of paths on which the product is ITM at time t (a=ITM), or equal to all the paths at time t (a=ALL). At time t, at path l, $U_t(l)$ has the form

$$U_t(l) = M(t)\frac{\mathrm{CF}(l;T)}{M(T)},$$

and by approximating $U_t(l)$ at every path l and every time step with the regression function $f_t(l)$, we obtain approximations of the discounted portfolio values for every path and every time step, resulting in an EPE profile

obtained by the LSMC method.

We start with implementing the LSMC method where the regression is based on the ITM paths only.

LSMC method (ITM paths case)

First we analyze the case where we only take the ITM paths in the regression. In Figure 3.1 (and Figure D.1 in Appendix D), we can see EPE profiles obtained by making use of the LSMC method (ITM paths case), for various strike prices.

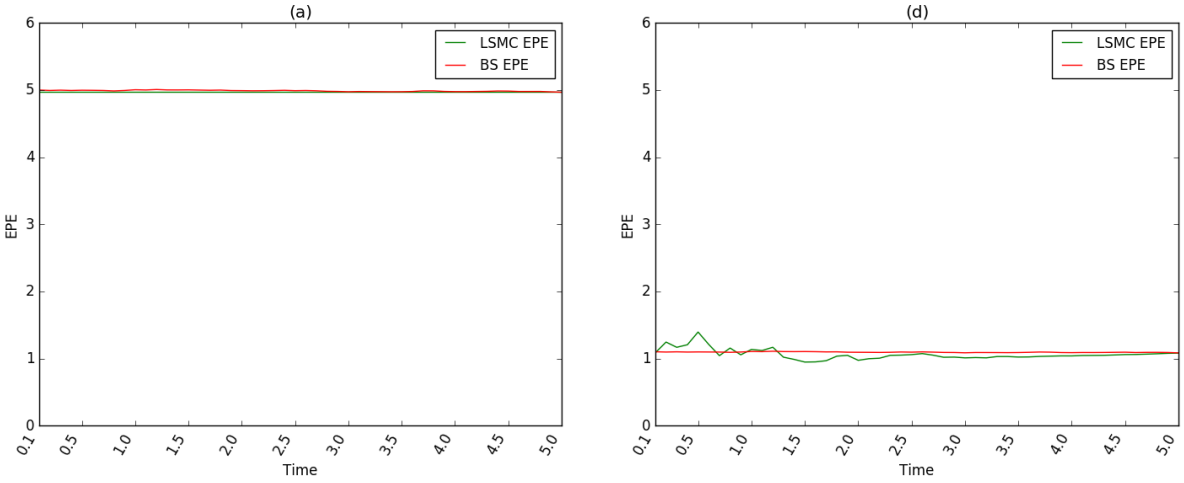

Figure 3.1: Figure where the EPE profiles by the LSMC method are compared to the EPE profile by Black-Scholes. Note that in the LSMC method, we based the regression on the ITM paths only, at every time step. Graph **(a)** shows the case where the strike price K is equal to zero, while graph **(d)** shows the case where $K = 5$. See Figure D.1 in Appendix D, for the EPE profiles where $K = 4$ and $K = 4.5$, shown in graphs **(b)** and **(c)** respectively.

By looking at Figure 3.1 and Figure D.1 in Appendix D, we can see that for higher values of K, the EPE profile by the LSMC method (ITM paths case) becomes less accurate (compared to the EPE profile generated by Black -Scholes). For higher values of K, more paths are left out in the regression at every time step, because the amount of ITM paths decreases.
At these paths that are left out, we obtain the approximations of the discounted portfolio values by making use of the regression based on the ITM paths only, which do not result in accurate estimations.

Now we take a look at the case of K being equal to $S(0)$. In Figure 3.2 we can see graphs showing how the regression fits the data, at different stages in time.

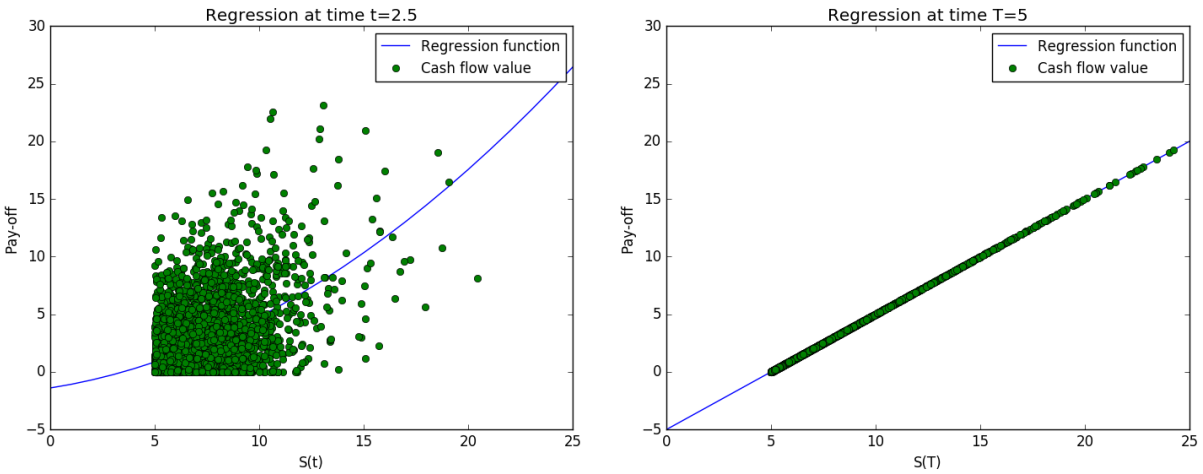

Figure 3.2: Examples of the regression in the LSMC method, at different times. In this setting, K is equal to $S(0)$, and only the ITM paths are taken into account at every time step in the regression.

We can note that at time $T = 5$, which is the maturity of the European call option, that when we only consider the ITM paths in our regression, we obtain a perfect estimation. This can be seen in Figure **(d)** in 3.1, where at time T, the EPE value by the Black-Scholes method is well approximated by the EPE value by the LSMC method. At time $t = 2.5$, the regression does not work optimally, because of the inaccurate approximations of the paths that are not ITM (which is approximated by the regression function based on the ITM paths only).

Now we are going to generate EPE profiles where in the LSMC method the regression is based on all paths.

LSMC method (all paths case)

In Figure 3.3 (and Figure E.1 in Appendix E), we can see EPE profiles obtained by making use of the LSMC method (all paths case), for multiple strike prices.

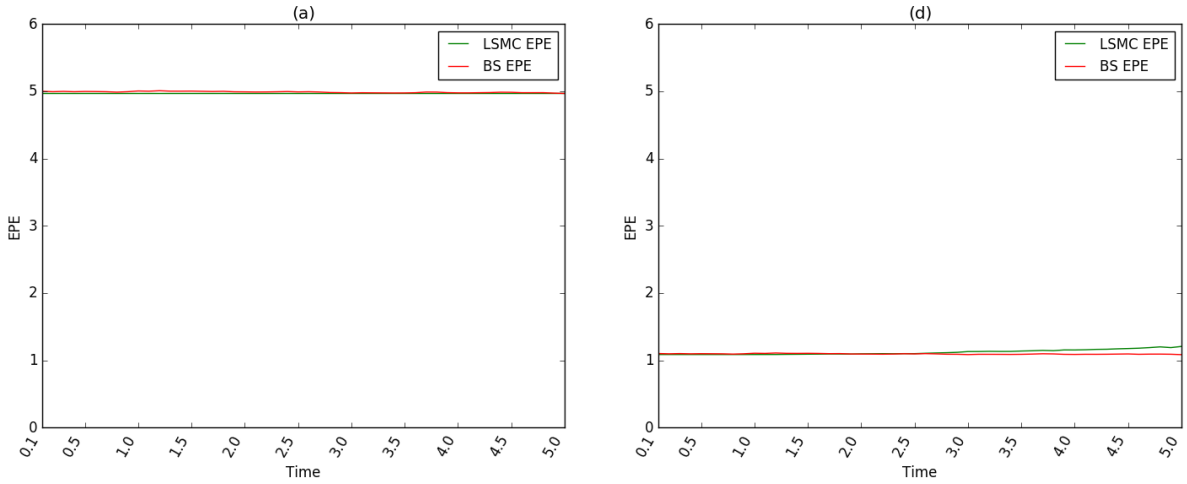

Figure 3.3: Figure where the EPE profiles by the LSMC method are compared to the EPE profile by Black-Scholes. Note that in the LSMC method, we based the regression on all the paths, at every time step. Graph **(a)** shows the case where the strike price K is equal to zero, while graph **(d)** shows the case where $K = 5$. See Figure D.1 in Appendix D, for the EPE profiles where $K = 4$ and $K = 4.5$, shown in graphs **(b)** and **(c)** respectively.

By looking at Figure 3.3 and Figure E.1 in Appendix E, we can see that for higher values of K, the EPE profile by the LSMC method (all paths case) becomes less accurate (compared to the EPE profile generated by Black-Scholes).

Now we take a look at the case of K being equal to $S(0)$. In Figure 3.4 we can see graphs showing how the regression fits the data, at different stages in time.

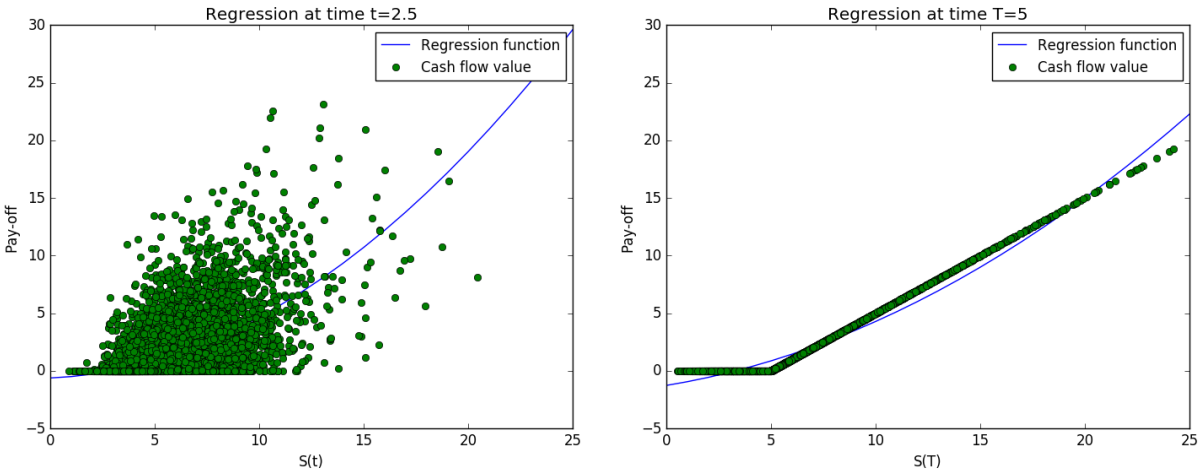

Figure 3.4: Examples showing the regression in the LSMC method, at different times. In this setting, K is equal to $S(0)$, and all the paths are taken into account at every time step in the regression.

We can note that at $T = 5$, which is the maturity of the European call option, that when we take all the paths in our regression, we do not obtain a perfect estimation as in the ITM paths case in Figure 3.2. This can be seen in graph **(d)** in Figure 3.3, where at time T the EPE value of the Black-Scholes method is not accurately approximated by the EPE value of the LSMC method. At time $t = 2.5$, the regression does better fit the discounted portfolio values, which we also see in graph **(d)** in Figure 3.3. This is caused by the fact that all the paths are taken into account in the regression, which approximates the discounted portfolio values more accurately.

In terms of making the choice of taking all the paths or just the ITM paths in the regression, we can see that no choice results in EPE profiles that are always more accurate. At last we take a look at the case where $K = 6$, which means that when the regression is based on the ITM paths only, a lot of paths are left out at every regression step. See Figure 3.5 for the EPE profiles for both the cases where the regression is based on the ITM paths only and the regression based on all the paths.

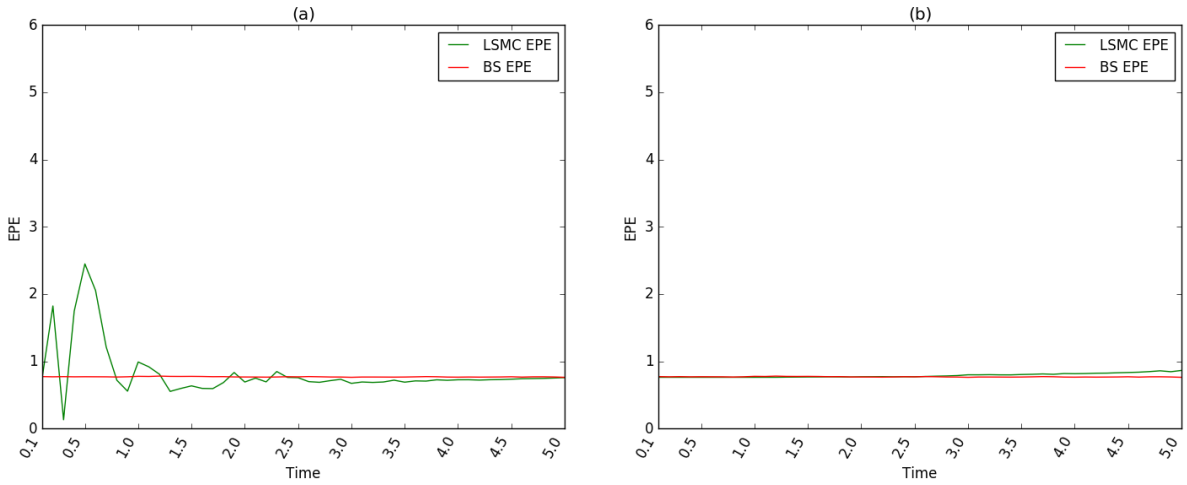

Figure 3.5: Graphs showing the EPE profiles by the LSMC method in the case when $K = 6$, for both the cases where the regression is based on the ITM paths only (graph **(a)**) and where the regression is based on all paths (graph **(b)**).

K	0	4	4.5	5	6
MSE (ITM paths case)	0.00051	0.00208	0.00266	0.00699	0.15032
MSE (all paths case)	0.00051	0.00218	0.00239	0.00251	0.00256

Table 3.1: MSE calculated for different strike prices, for the EPE profiles obtained by different approaches in the regression in the LSMC method.

Furthermore, looking at Table 3.1, where the MSE is calculated for different strike prices, we can note that the LSMC method where the regression is based on the ITM paths only does not perform well when $K = 6$. We can conclude that we prefer to use the LSMC method in the case where the regression is based on all the paths, to generate EPE profiles in the uncollateralized case.

In Section 3.2.2 we take a look at the fully collateralized case, where we generate EPE profiles in the presence of the MPoR.

3.2.2 Fully collateralized case

In this section we are going to generate EPE profiles in the presence of the MPoR, which is the general aim for this thesis. We start with the formula for the EPE at time t, in the fully collateralized case:

$$\begin{aligned}\mathrm{EPE}(t) &= \mathbb{E}\left[\left(M(0)\frac{V(t)}{M(t)} - M(0)\frac{V(t-\delta)}{M(t-\delta)}\right)^+\right] \\ &\approx \mathbb{E}\left[\left(M(0)\frac{f_t(x)}{M(t)} - M(0)\frac{f_{t-\delta}(x-\delta)}{M(t-\delta)}\right)^+\right].\end{aligned}$$

As in the uncollateralized case, the portfolio value at time t, at every path, is approximated by the regression function $f_t(x)$ in (3.2). The MPoR occurs in the time interval $[t-\delta, t]$ and has a duration of δ, as in previous chapters. δ is chosen to be equal to 0.1, which is equal to the size of the time step.

We start with taking a close look at a specific case, where the strike price K is equal to zero. The reason behind this is because we can obtain the value of the EPE at time t in this setting analytically:

$$\begin{aligned}\mathrm{EPE}(t) &= \mathbb{E}\left[\left(\frac{V(t)}{M(t)} - \frac{V(t-\delta)}{M(t-\delta)}\right)^+\right] \\ &\overset{(a)}{=} \mathbb{E}\big[(S(t) - S(t-\delta))^+\big] \\ &= \mathbb{E}\big[(S(0)\cdot e^{-\frac{1}{2}\sigma^2 t + \sigma W_t} - S(0)\cdot e^{-\frac{1}{2}\sigma^2(t-\delta)+\sigma W_{t-\delta}})^+\big] \\ &= \mathbb{E}\big[S(0)\cdot e^{-\frac{1}{2}\sigma^2 t}(e^{\sigma W_t} - e^{\frac{1}{2}\sigma^2\delta + \sigma W_{t-\delta}})^+\big] \\ &= S(0)\cdot e^{-\frac{1}{2}\sigma^2 t}\cdot\mathbb{E}\big[(e^{\sigma W_t} - e^{\frac{1}{2}\sigma^2\delta+\sigma W_{t-\delta}})^+\big] \\ &= S(0)\cdot e^{-\frac{1}{2}\sigma^2 t}\cdot\mathbb{E}\big[e^{\sigma W_{t-\delta}}(e^{\sigma(W_t - W_{t-\delta})} - e^{\frac{1}{2}\sigma^2\delta})^+\big] \\ &\overset{(b)}{=} S(0)\cdot e^{-\frac{1}{2}\sigma^2 t}\cdot\mathbb{E}\big[e^{\sigma W_{t-\delta}}\big]\cdot\mathbb{E}\big[(e^{\sigma(W_t - W_{t-\delta})} - e^{\frac{1}{2}\sigma^2\delta})^+\big] \\ &\overset{(c)}{=} S(0)\cdot e^{-\frac{1}{2}\sigma^2 t}\cdot e^{\frac{1}{2}\sigma^2(t-\delta)}\cdot\mathbb{E}\big[(e^{\sigma(W_t - W_{t-\delta})} - e^{\frac{1}{2}\sigma^2\delta})^+\big] \\ &= S(0)\cdot e^{-\frac{1}{2}\sigma^2\delta}\cdot\mathbb{E}\big[(e^{\sigma(W_t - W_{t-\delta})} - e^{\frac{1}{2}\sigma^2\delta})^+\big]\end{aligned}$$

$$
\begin{aligned}
&\overset{(d)}{=} S(0)\cdot e^{-\frac{1}{2}\sigma^2\delta}\cdot\mathbb{E}\big[(e^{\sigma\sqrt{\delta}Z}-e^{\frac{1}{2}\sigma^2\delta})^+\big]\\
&\overset{(e)}{=} S(0)\cdot e^{-\frac{1}{2}\sigma^2\delta}\cdot\int_{\frac{1}{2}\sigma\sqrt{\delta}}^{\infty}\big[e^{\sigma\sqrt{\delta}z}-e^{\frac{1}{2}\sigma^2\delta}\big]\frac{1}{\sqrt{2\pi}}e^{-\frac{1}{2}z^2}dz\\
&\overset{(f)}{=} S(0)\cdot e^{-\frac{1}{2}\sigma^2\delta}\cdot\Bigg(\underbrace{\int_{\frac{1}{2}\sigma\sqrt{\delta}}^{\infty}e^{\sigma\sqrt{\delta}z}\frac{1}{\sqrt{2\pi}}e^{-\frac{1}{2}z^2}dz}_{(1)}-\underbrace{\int_{\frac{1}{2}\sigma\sqrt{\delta}}^{\infty}e^{\frac{1}{2}\sigma^2\delta}\frac{1}{\sqrt{2\pi}}e^{-\frac{1}{2}z^2}dz}_{(2)}\Bigg)\\
&= S(0)\cdot e^{-\frac{1}{2}\sigma^2\delta}\cdot\Big[e^{\frac{1}{2}\sigma^2\delta}\cdot\Big(1-\Phi\Big(-\frac{1}{2}\sigma\sqrt{\delta}\Big)\Big)-e^{\frac{1}{2}\sigma^2\delta}\cdot\Big(1-\Phi\Big(\frac{1}{2}\sigma\sqrt{\delta}\Big)\Big)\Big]\\
&\overset{(g)}{=} S(0)\cdot\Big(-\Phi\Big(-\frac{1}{2}\sigma\sqrt{\delta}\Big)+\Phi\Big(\frac{1}{2}\sigma\sqrt{\delta}\Big)\Big) \qquad (3.3)
\end{aligned}
$$

with the following remarks:

(a) The portfolio consists of just one European call option with strike $K = 0$, which results in the value of the portfolio at time t being equal to the value of the underlying stock at time t. Furthermore, we assumed that the annual interest rate r is equal to zero, so the numeraire $M(t)$ is equal to 1 for every time t.

(b) Note that the random variables $e^{\sigma W_{t-\delta}}$ and $(e^{\sigma(W_t-W_{t-\delta})}-e^{\frac{1}{2}\sigma^2\delta})^+$ are independent random variables, which means we can split the expectation in two parts.

(c) $e^{\sigma W_{t-\delta}} \sim \mathrm{LN}(0,\sigma^2(t-\delta))$, which means that $\mathbb{E}[e^{\sigma W_{t-\delta}}] = e^{\frac{1}{2}\sigma^2(t-\delta)}$.

(d) $W_t - W_{t-\delta} \sim \mathcal{N}(0,\delta)$, so we can substitute $W_t - W_{t-\delta}$ with $\sqrt{\delta}Z$ in the expectation, where $Z \sim \mathcal{N}(0,1)$.

(e) To obtain the lower boundary for the integral, we solve the following equation:

$$e^{\sigma\sqrt{\delta}Z} - e^{\frac{1}{2}\sigma^2\delta} = 0$$

if and only if

$$\sigma\sqrt{\delta}Z - \frac{1}{2}\sigma^2\delta = 0$$

if and only if

$$Z = \frac{1}{2}\sigma\sqrt{\delta}.$$

We can conclude that the expectation is greater than zero when $Z > \frac{1}{2}\sigma\sqrt{\delta}$, which will be the lower boundary of the integral.

(f) See Appendix C for the solution of these integral (1) and (2).

(g) Note that $-\Phi\Big(-\frac{1}{2}\sigma\sqrt{\delta}\Big) + \Phi\Big(\frac{1}{2}\sigma\sqrt{\delta}\Big)$ is the inner part of the standard normal probability density function, integrated in the interval $[-\frac{1}{2}\sigma\sqrt{\delta}, \frac{1}{2}\sigma\sqrt{\delta}]$. See for an illustration Figure 3.6.

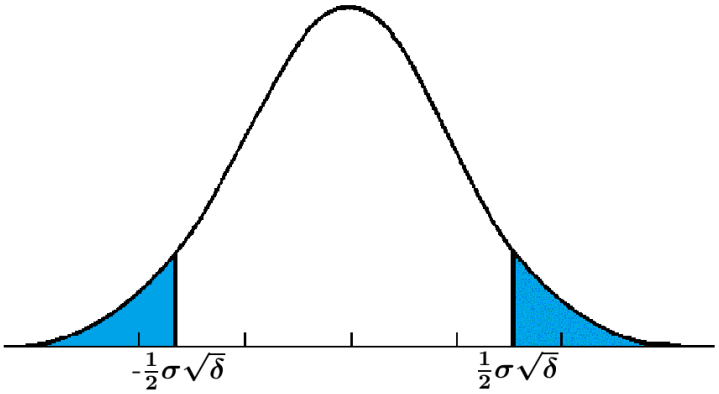

Figure 3.6: Standard normal probability density function where we integrate in the interval $[-\frac{1}{2}\sigma\sqrt{\delta}, \frac{1}{2}\sigma\sqrt{\delta}]$.

In Figure 3.7 we see the EPE profiles generated by Black-Scholes and equation (3.3).

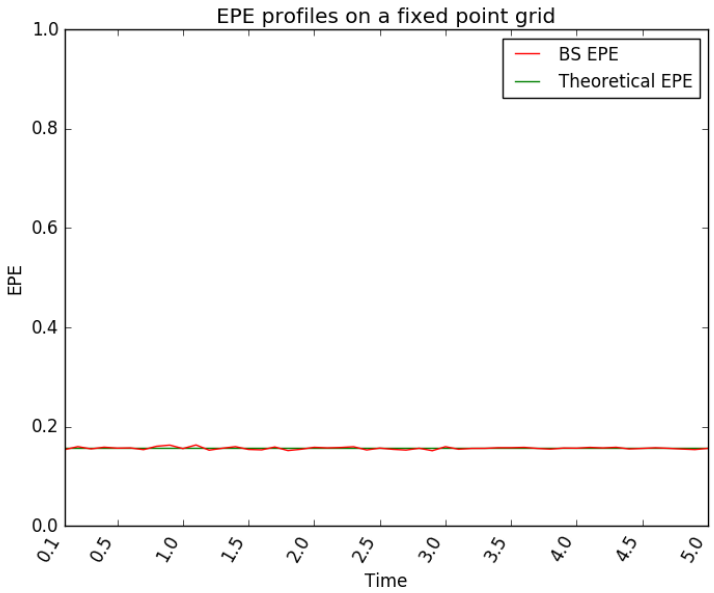

Figure 3.7: Graph of the EPE profiles generated by Black-Scholes and by equation (3.3). The portfolio consists of a European call option with strike equal to zero, which corresponds to a portfolio containing one stock. Time steps are chosen to be 0.1, which is equal to the duration of the MPoR, δ.

Now we are going to generate EPE profiles where in the LSMC method we only take the ITM paths at every step in the regression. In the setting where the strike price K is equal to zero, we make use of the analytical EPE profile, where the value of the EPE is shown in (3.3).

LSMC method (ITM paths case)

In Figure 3.8 (and Figure D.2 in Appendix E), we can see EPE profiles obtained by making use of the LSMC method (ITM paths case), for various strike prices.

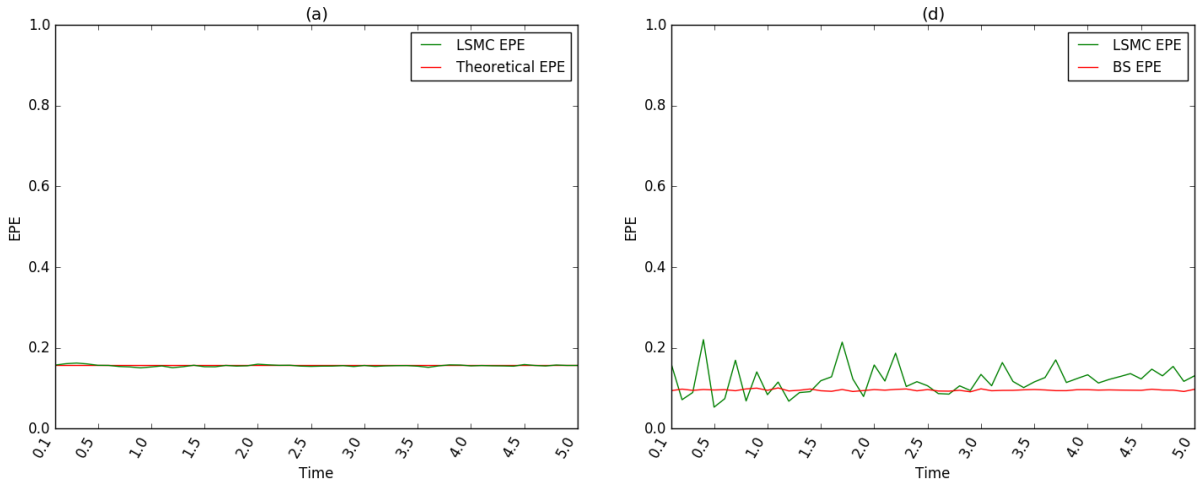

Figure 3.8: Figure where the EPE profiles by the LSMC method are compared to the EPE profile by Black-Scholes (when $K = 0$ compared with equation (3.3)). Note that in the LSMC method, we based the regression on the ITM paths only, at every time step. Graph **(a)** shows the case where the strike price K is equal to zero, while graph **(d)** shows the case where $K = 5$. See Figure D.2 in Appendix D, for the EPE profiles where $K = 4$ and $K = 4.5$, shown in graphs **(b)** and **(c)** respectively. Time steps are chosen to be 0.1, which is equal to the duration of the MPoR, δ.

By looking at Figure 3.8 and Figure D.2 in Appendix D, we can see that for higher values of K, the EPE profile by the LSMC method (ITM paths case) becomes less accurate. For higher values of K, more paths are left out in the regression at every time step, because the amount of ITM paths decreases. At these paths that are left out, we obtain the approximations of the discounted portfolio values by making use of the regression based on the ITM paths only, which do not result in accurate estimations.

Note that we do not take a look at the regression performance plots as we did in the uncollateralized case, because the regression stays the same, only the formula of the EPE profile changes.

Now we are going to generate EPE profiles where in the LSMC method the regression is based on all paths. In the setting where the strike price K is equal to zero, we make use of the analytical EPE profile in (3.3).

LSMC method (all paths case)

In Figure 3.9 (and Figure E.2 in Appendix E), we can see EPE profiles obtained by making use of the LSMC method (all paths case), for multiple strike prices.

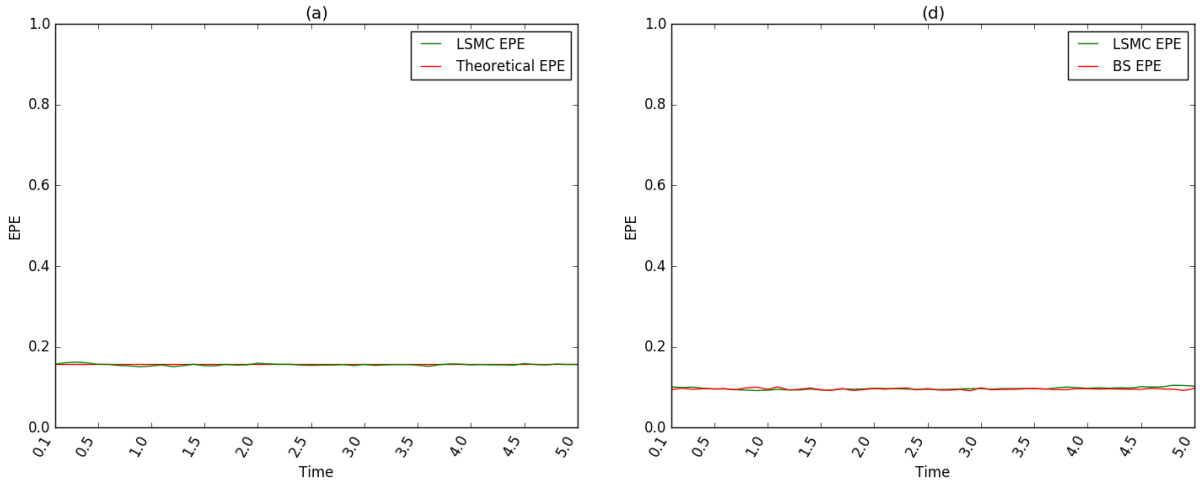

Figure 3.9: Figure where the EPE profile by the LSMC method is compared to the EPE profile by Black-Scholes (when $K = 0$ compared with equation (3.3)). Note that in the LSMC method, we based the regression on all the paths, at every time step. Graph **(a)** shows the case where the strike price K is equal to zero, while graph **(d)** shows the case where $K = 5$. See Figure D.1 in Appendix D, for the EPE profiles where $K = 4$ and $K = 4.5$, shown in graphs **(b)** and **(c)** respectively. Time steps are chosen to be 0.1, which is equal to the duration of the MPoR, δ.

By looking at Figure 3.9 and Figure E.2 in Appendix E, we can see that for higher values of K, the EPE profile created by the LSMC method (all paths case) becomes less accurate (compared to the EPE profile by Black-Scholes).

In terms of making the choice of taking all the paths or just the ITM paths in the regression, we can clearly see in the figures that the LSMC method produces more accurate EPE profiles when the regression is based on all the paths. Furthermore, in Figure 3.10 the EPE profiles are shown where $K = 6$, in the cases where the regression is based on the ITM paths only (graph **(a)**) and when the regression is based on all the paths (graph (b)). We can see that when more paths are left out at every regression step, the resulting EPE profile gets more inaccurate. In Table 3.2 the MSE is calculated for different

strike prices, where we can see that when the regression is based on the ITM paths only, we obtain far less accurate results compared to when all the paths are taken into account in the regression.

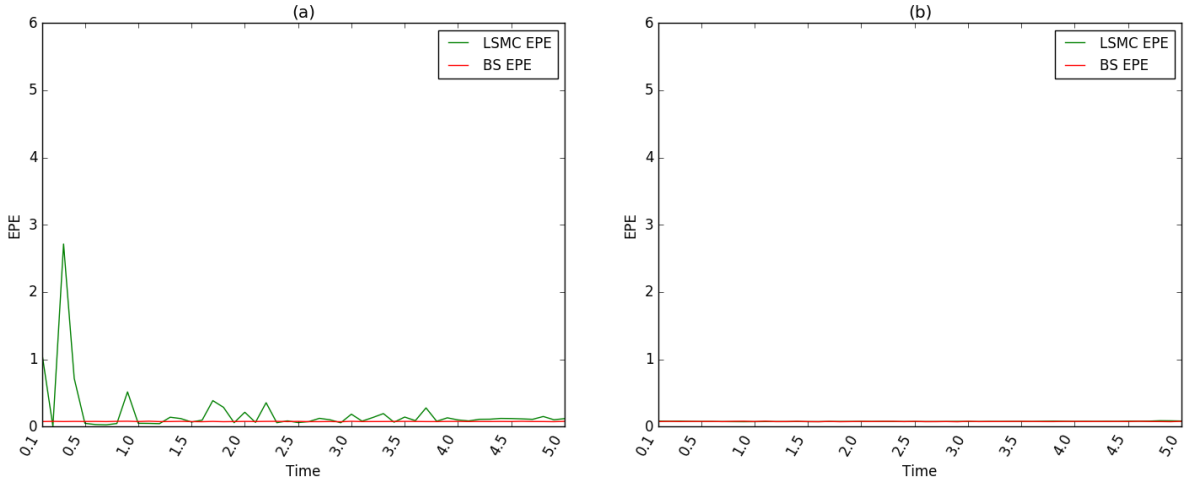

Figure 3.10: Graphs showing the EPE profiles by the LSMC method in the case when $K = 6$, for both the cases where the regression is based on the ITM paths only (graph **(a)**) and where the regression is based on all paths (graph **(b)**). Time steps are chosen to be 0.1, which is equal to the duration of the MPoR, δ.

K	0	4	4.5	5	6
MSE (ITM paths case)	0.00001	0.00032	0.00067	0.00183	0.17815
MSE (all paths case) $(\cdot 10^{-5})$	1.07835	1.42595	1.51070	1.52775	1.47761

Table 3.2: MSE calculated for different strike prices K, for the EPE profiles obtained by different approaches in the regression in the LSMC method.

We can conclude that we prefer to use the LSMC method in the case where the regression is based on all the paths at every time step, in order to generate accurate EPE profiles in the fully collateralized case. This means that in both the uncollateralized and the fully collateralized case, taking all the paths in the regression at every time step is preferred in terms of generating accurate EPE profiles.

Chapter 4

Conclusion

The aim of this thesis is to model fully collateralized exposures in the presence of the MPoR. We start with introducing a closed-form expression that is used to generate EPE profiles in the setting of having a portfolio containing a fixed versus floating interest rate swap. We made use of the open source software ORE, that is able to generate EPE profiles in the presence of the MPoR.

With a calibration method we were able to generate EPE profiles with the closed-form expression, and compared these with EPE profiles generated by ORE. This approach allows us to obtain reliable EPE profiles in the case where we use daily simulation, as outlined in Section 2.3.

We then applied the Brownian bridge method as introduced in Section 2.4, which lets us avoid daily simulation of discounted portfolio values. The method consists of constructing a Brownian bridge between two portfolio values at different times (which are obtained by simulation with ORE), on a time grid where the time step size is larger than daily. The implementation of the standard Brownian bridge method resulted in inaccurate EPE profiles[1], because of the cash flows occurring between the portfolio values we applied the Brownian bridge method to. The new Brownian bridge method deals with this problem, by only applying the Brownian bridge method between portfolio values where no cash flows occur in between. For both methods we show results and discuss the performance. We have studied the Brownian bridge method in a simplified setting and shown empirically that the performance of this methodology is linked to how the cash flows of the portfolio are being treated.

We then resort to modeling the MPoR in the setting where discounted port-

[1]This method is stated in [5] (see Section 8.2 therein), but adjusted to our own setting.

folio values are approximated by the LSMC method. This method uses regression functions to estimate the discounted portfolio values at every time step. The LSMC method tackles the problem of dealing with a portfolio consisting of products that cannot be valued analytically at each time step. We work in a Black-Scholes setting, where we consider a portfolio consisting of one European call option.

In this setting we generated EPE profiles where we started in the uncollateralized case, where the distinction is made in terms of regressing on only the ITM paths or on all the paths, at every time step. We showed figures where the regression is shown at different times in both the cases of regressing on the ITM paths or on all the paths. For the uncollateralized case, we made the conclusion that when in the LSMC method the regression is based on all paths we result in more accurate EPE profiles, compared to the EPE profiles obtained by regressing on the ITM paths only.

For the fully collateralized case, where we model the MPoR, we started with a special case of setting the strike price to zero, and obtained an analytical solution for the EPE at every time step. We then generated EPE profiles with the distinction between regressing on only the ITM paths or on all the paths, at every time step. For the fully collateralized case, we concluded that the choice of regressing on all the paths at every time step results in more accurate EPE profiles, compared to the EPE profiles obtained by regressing on the ITM paths only.

We made the conclusion that for both the uncollateralized and the fully collateralized case, regressing on all the paths results in more accurate EPE profiles compared to the EPE profiles obtained by regressing on the ITM paths only.

As a general conclusion, we state that we are able to use three different methods for obtaining discounted portfolio values that allows us to generate EPE profiles in the presence of the MPoR. These methods consists of making use of crude Monte Carlo simulation only, making use of crude Monte Carlo simulation combined with the Brownian bridge method, or making use of the LSMC method. For a portfolio containing a fixed versus floating interest swap, we have investigated how EPE profiles can be generated by either making use of crude Monte Carlo simulation only or by making use of crude Monte Carlo simulation combined with the Brownian bridge method. We concluded that we only make use of crude Monte Carlo simulation of discounted portfolio values when we do not require high computational costs, and the Brownian bridge method helps to reduce these computational costs, while still obtaining accurate EPE profiles. For a portfolio containing an European call option in a Black-Scholes setting, we have generated EPE profiles

by making use of Black-Scholes or by the LSMC method. We concluded that the LSMC method does generate accurate EPE profiles when the regression is based on all paths at every time step. We have not extended the LSMC to the fixed versus floating interest rate swap case, which is left for further research.

For further research we suggest that EPE profiles are generated by the LSMC method in the case of a fixed versus floating interest rate swap, with the same time discretization points on the grid. This allows us to directly compare the EPE profiles obtained by crude Monte Carlo simulation and by the LSMC method. Furthermore, the Brownian bridge method can be applied together with the LSMC method, which could improve the computation time of the simulation.

Appendix A

Analytic formula for the value of an interest rate swap

Value at time t of a payer interest rate swap, with $0 \leq t \leq u$, observation date u fixed, of cash flows occurring after u:

$$\begin{aligned}
V(t) &= N \cdot [y(t) - K] \cdot \text{pvbp}_{i(u)}(t) \\
&= N \cdot \left[\frac{\sum_{j=k(u)}^{m} \tau_j^{\text{flt}} \cdot F(t, \bar{T}_{j-1}^{\text{flt}}, \bar{T}_j^{\text{flt}}) \cdot P(t, \bar{T}_j^{\text{flt}})}{\text{pvbp}_{i(u)}(t)} - K \right] \cdot \text{pvbp}_{i(u)}(t) \\
&= N \cdot \left[\sum_{j=k(u)}^{m} \tau_j^{\text{flt}} \cdot F(t, \bar{T}_{j-1}^{\text{flt}}, \bar{T}_j^{\text{flt}}) \cdot P(t, \bar{T}_j^{\text{flt}}) - K \cdot \text{pvbp}_{i(u)}(t) \right] \\
&= N \cdot \left[\sum_{j=k(u)}^{m} \tau_j^{\text{flt}} \cdot F(t, \bar{T}_{j-1}^{\text{flt}}, \bar{T}_j^{\text{flt}}) \cdot P(t, \bar{T}_j^{\text{flt}}) - K \cdot \sum_{j=i(u)}^{n} \tau_j^{\text{fix}} \cdot P(t, \bar{T}_j^{\text{Fix}}) \right],
\end{aligned}$$

with $i(u) = \min_i \{\bar{T}_i^{\text{fix}} > u\}$ and $k(u) = \min_k \{\bar{T}_k^{\text{flt}} > u\}$. We can see that the value of this interest rate swap can be seen as the sum of all floating cash flows received from the counterparty, minus the sum of all fixed cash flows we pay to the counterparty.

Appendix B

Specification of ORE files

The specifications of the input and output files used in ORE:

ORE Input files

ore_mpor.xml	: Master input file;
portfolio.xml	: Trade data;
netting_mpor.xml	: Collateral (CSA) data;
simulation.xml	: Configuration of simulation model and market;
market.txt	: Market data snapshot on 5-Feb-2016;
fixings.txt	: Index fixings history;
curveconfig.xml	: Curve and term structure composition from individual market instruments;
conventions.xml	: Market conventions for all market data points;
todaysmarket.xml	: Configuration of the market composition, relevant for the pricing of the given portfolio as of today (yield curves, FX rates, volatility surfaces etc);
pricingengines.xml	: Configuration of pricing methods by product.

Swap specifications

start date	: 5-Feb-2016;
end date	: 6-Feb-2021;
Currency	: EUR;
K	: 0.01;
N	: 100;
Fix rate tenor	: 1Y;
Float rate tenor	: 3M.

Simulation

Discretization	: Exact;
Grid	: 1210 x 1D;
Samples	: 300.

CSA

Threshold pay	: 0;
Threshold receive	: 0;
MTA pay	: 0;
MTA receive	: 0;
Call Frequency	: 1D;
Post Frequency	: 1D;
MPoR (δ)	: 10D.

ORE output files

netcube.csv	: NPV cube after netting and collateral;
exposure_nettingset_$*$.csv	: Netting set exposure evolution reports;
curves.csv	: Generated yield (discount) curves report.

Appendix C

Solution of integrals

The integrals (1) and (2) in equation (3.3) solved:

(1):

$$\begin{aligned}\int_{\frac{1}{2}\sigma\sqrt{\delta}}^{\infty} e^{\sigma\sqrt{\delta}z}\frac{1}{\sqrt{2\pi}}e^{-\frac{1}{2}z^2}dz &= \int_{\frac{1}{2}\sigma\sqrt{\delta}}^{\infty}\frac{1}{\sqrt{2\pi}}e^{-\frac{1}{2}z^2+\sigma\sqrt{\delta}z}dz\\ &= \int_{\frac{1}{2}\sigma\sqrt{\delta}}^{\infty}\frac{1}{\sqrt{2\pi}}e^{-\frac{1}{2}(z-\sigma\sqrt{\delta})^2+\frac{1}{2}\sigma^2\delta}dz\\ &= e^{\frac{1}{2}\sigma^2\delta}\int_{\frac{1}{2}\sigma\sqrt{\delta}}^{\infty}\frac{1}{\sqrt{2\pi}}e^{-\frac{1}{2}(z-\sigma\sqrt{\delta})^2}dz\\ &= e^{\frac{1}{2}\sigma^2\delta}\int_{-\frac{1}{2}\sigma\sqrt{\delta}}^{\infty}\frac{1}{\sqrt{2\pi}}e^{-\frac{1}{2}y^2}dy\\ &= e^{\frac{1}{2}\sigma^2\delta}\cdot\Big(1-\Phi\Big(-\frac{1}{2}\sigma\sqrt{\delta}\Big)\Big)\end{aligned}$$

(2):

$$\begin{aligned}\int_{\frac{1}{2}\sigma\sqrt{\delta}}^{\infty} e^{\frac{1}{2}\sigma^2\delta}\frac{1}{\sqrt{2\pi}}e^{-\frac{1}{2}z^2}dz &= e^{\frac{1}{2}\sigma^2\delta}\int_{\frac{1}{2}\sigma\sqrt{\delta}}^{\infty}\frac{1}{\sqrt{2\pi}}e^{-\frac{1}{2}z^2}dz\\ &= e^{\frac{1}{2}\sigma^2\delta}\cdot\Big(1-\Phi\Big(\frac{1}{2}\sigma\sqrt{\delta}\Big)\Big)\end{aligned}$$

Appendix D

EPE profiles (ITM paths case)

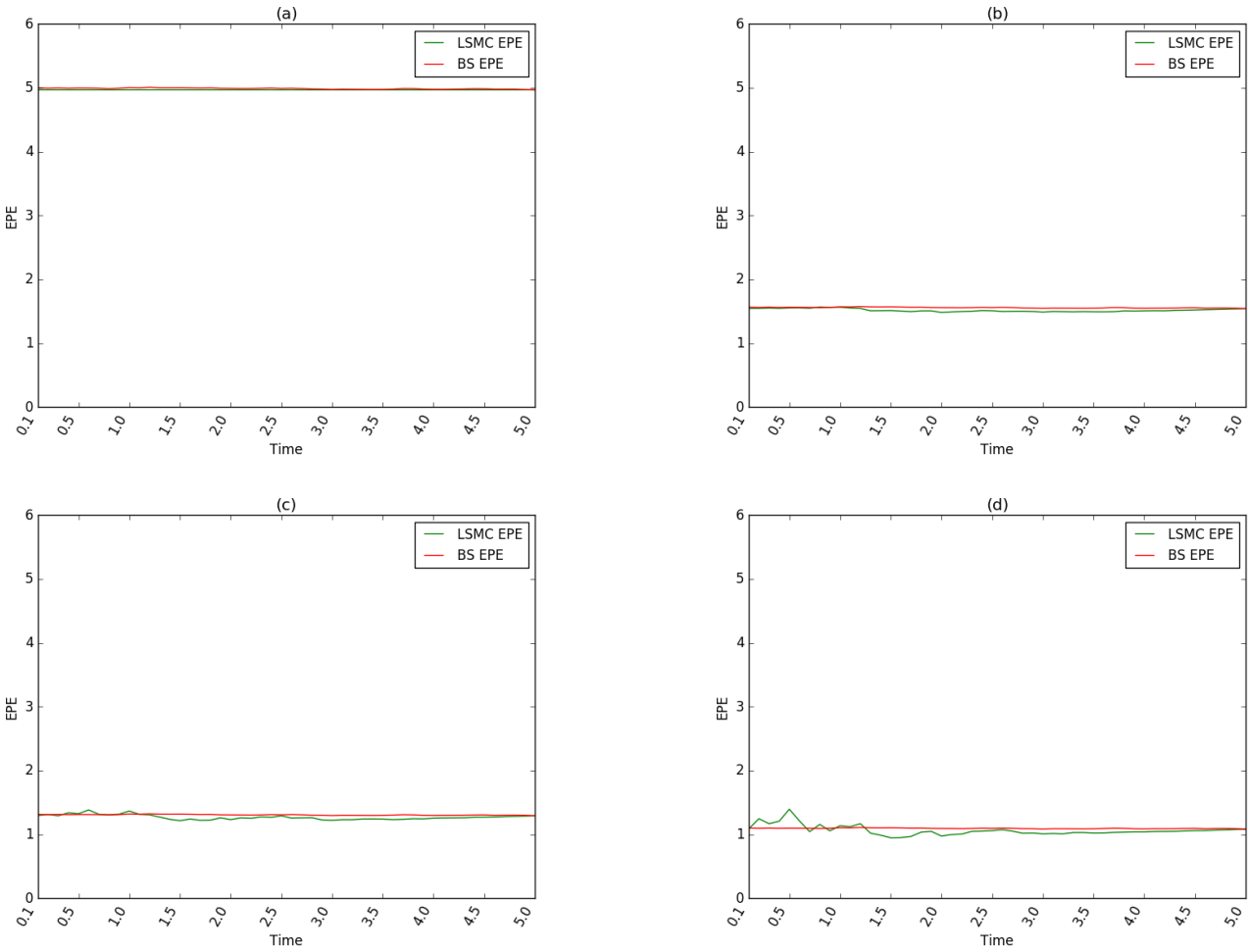

(c) $K = 4.5$ (d) $K = 5$

Figure D.1: EPE profiles in the uncollateralized case, with only ITM paths in the regression.

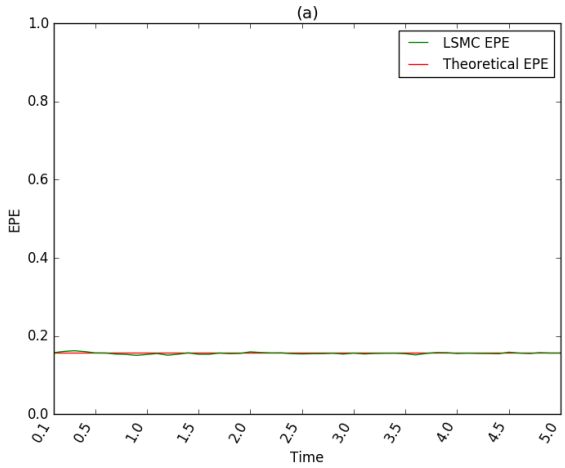

(a) $K = 0$

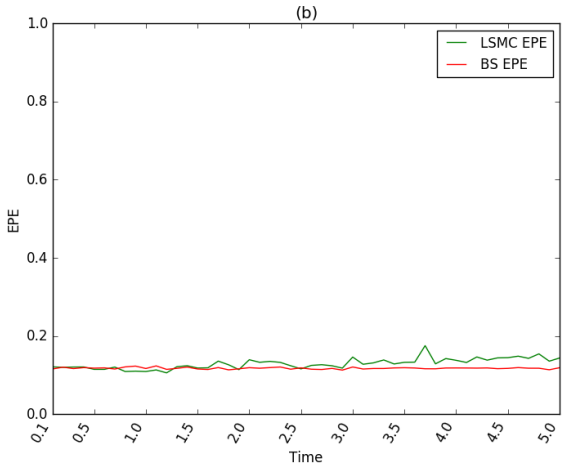

(b) $K = 4$

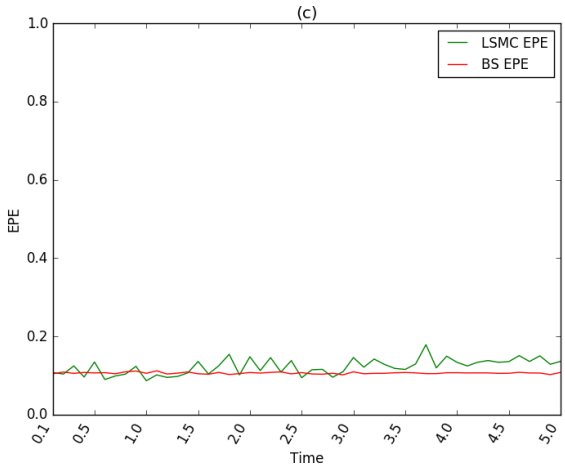

(c) $K = 4.5$

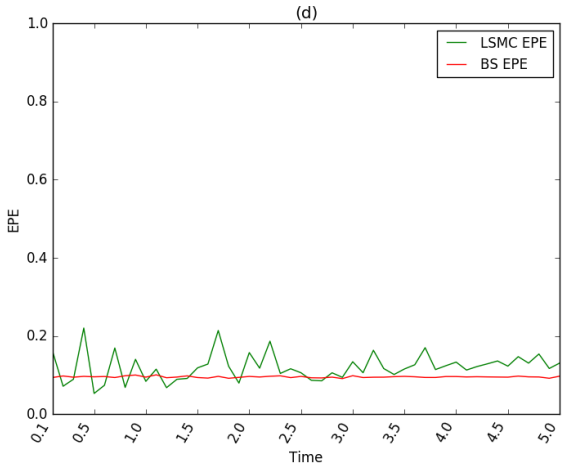

(d) $K = 5$

Figure D.2: EPE profiles in the fully collateralized case, with only ITM paths in the regression.

Appendix E

EPE profiles (all paths case)

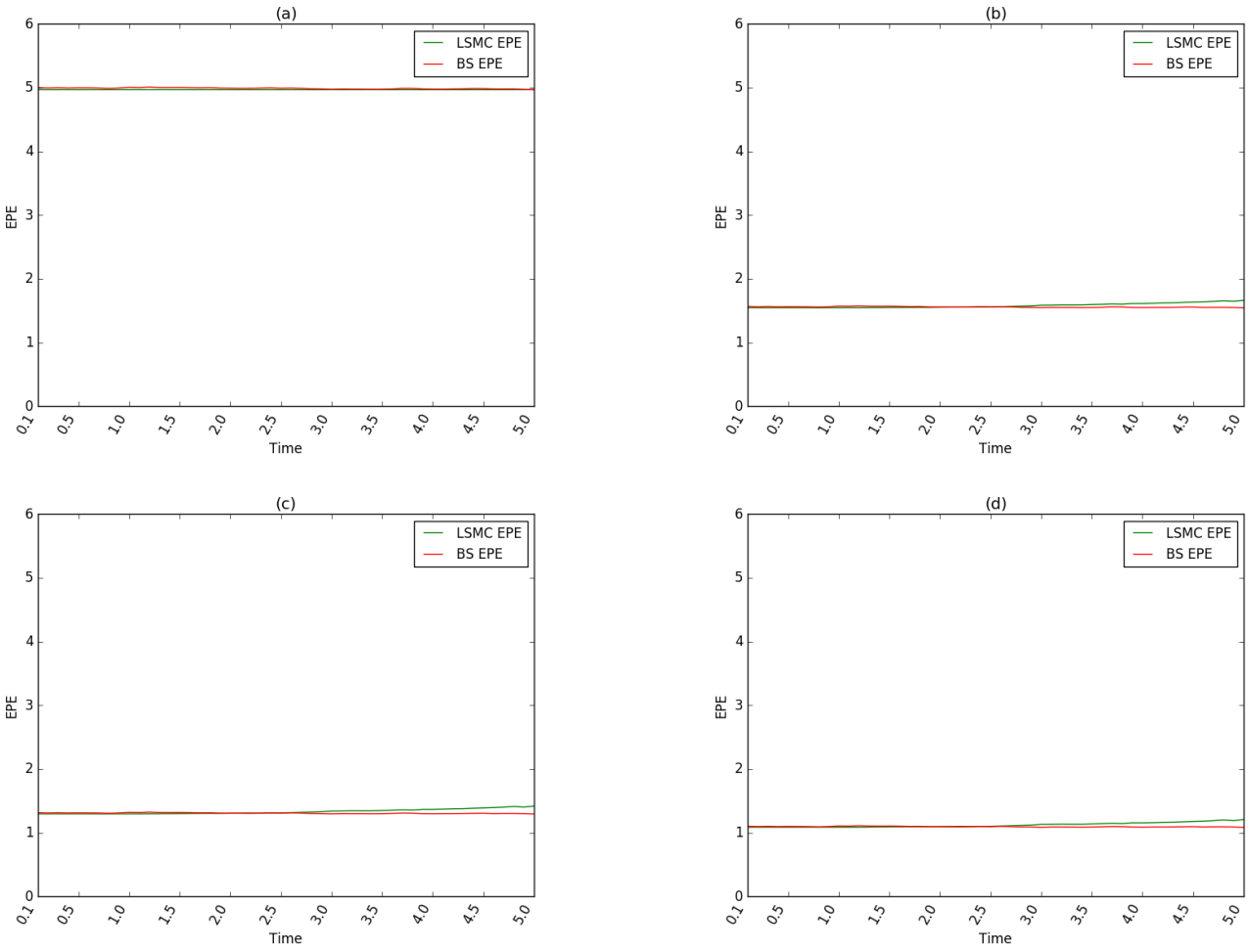

(c) $K = 4.5$ (d) $K = 5$

Figure E.1: EPE profiles in the uncollateralized case, with all the paths in the regression.

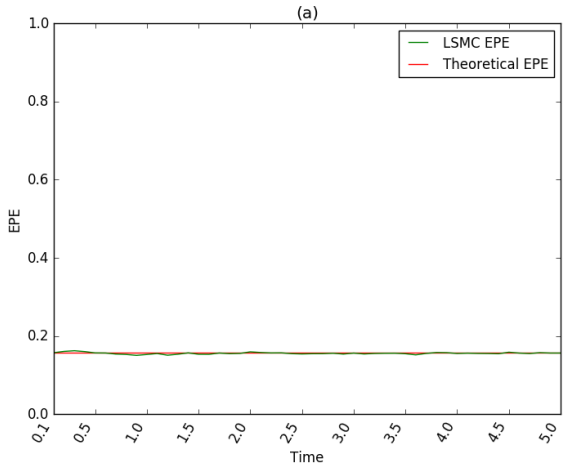

(a) $K = 0$

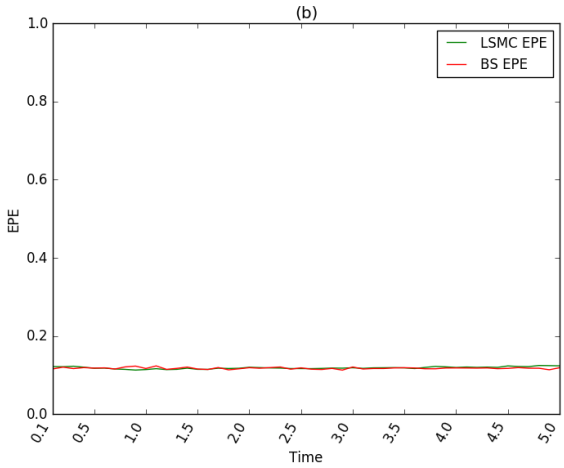

(b) $K = 4$

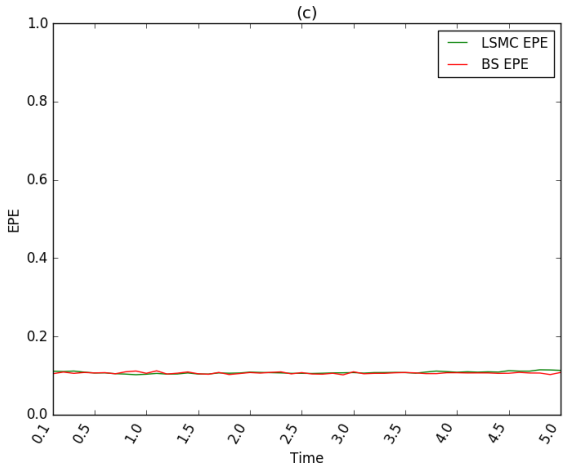

(c) $K = 4.5$

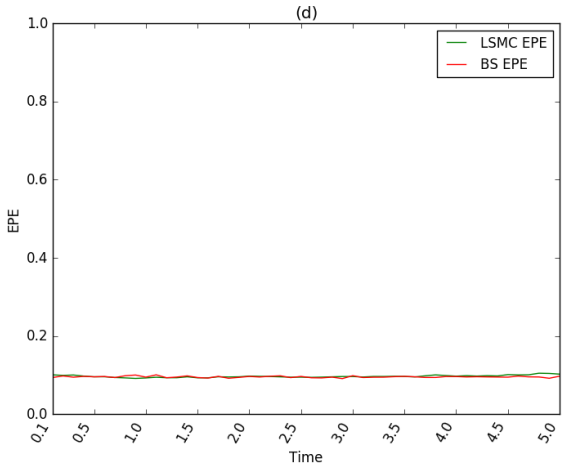

(d) $K = 5$

Figure E.2: EPE profiles in the fully collateralized case, with all the paths in the regression.

Bibliography

[1] D. Brigo, M. Morini, and A. Pallavicini, *Counterparty Credit Risk, Collateral and Funding with Pricing Cases for all Asset Classes.* Wiley Finance, 2013.

[2] M. Pykhtin and S. Zhu, "A guide to Modelling Counterparty Credit Risk," *GARP Risk Review*, July/August 2007.

[3] M. Joshi and O. Kang Kwon, "Least Squares Monte Carlo Credit Value Adjustment with Small and Unidirectional Bias," 2016.

[4] D. Lu, *The XVA of Financial Derivatives. CVA, DVA and FVA explained.* Palgrave macmillan, 2016.

[5] L. Andersen, M. Pykhtin, and A. Sokol, "Rethinking the Margin Period of Risk," *Journal of Credit Risk 13(1), 1-45*, 2017.

[6] P. Hunt and J. Kennedy, *Financial Derivatives in Theory and Practice.* Wiley, 2004.

[7] Quaternion, *ORE User Guide.* Quaternion Risk Management, April 2017.

[8] S. J. Sheather, "Density estimation," *Statistical Science, Vol. 19, No. 4 (Nov., 2004), pp. 588-597*, 2004.

[9] E. Nadaraya, "On estimating regression," 1964.

[10] P. Glasserman, *Monte Carlo Methods in Financial Engineering.* Springer, 2004.

[11] J.-F. Le Gall, *Brownian Motion, Martingales, and Stochastic Calculus.* Springer, 2016.

[12] R. Lichters, R. Stamm, and D. Gallagher, *Modern Derivatives Pricing and Credit Exposure Analysis.* Palgrave macmillan, 2015.

[13] F. A. Longstaff and E. S. Schwartz, "Valuing American Options by Simulation: A simple Least-Squares Approach," 2001.